

# $B_s \rightarrow PP$ decays and the NLO contributions in the pQCD Approach

Jing Liu, Rui Zhou and Zhen-Jun Xiao <sup>\*</sup>,

*Department of Physics and Institute of Theoretical Physics,  
Nanjing Normal University, Nanjing, Jiangsu 210097, P.R.China*

(Dated: November 2, 2021)

## Abstract

By employing the perturbative QCD(pQCD) factorization approach, we calculated the partial next-to-leading order (NLO) contributions to  $B_s \rightarrow PP$  decays ( $P = \pi, K, \eta^{(\prime)}$ ), coming from the QCD vertex corrections, the quark-loops and the chromo-magnetic penguins. we found numerically that (a) for three measured decays  $\bar{B}_s \rightarrow K^+\pi^-, K^+K^-$  and  $\pi^+\pi^-$ , the consistency between the pQCD predictions and the measured values are improved effectively by the inclusion of the NLO contributions; (b) for  $\bar{B}_s \rightarrow K^0\eta^{(\prime)}$  and  $K^0\pi^0$  decays, the NLO enhancements to the branching ratios can be significant, from  $\sim 50\%$  to  $170\%$ , to be tested by the LHC experiments; (c) for the CP-violating asymmetries, the leading order pQCD predictions can also be changed significantly by the inclusion of the NLO contributions; (d) for  $\bar{B}_s \rightarrow K^+\pi^-$  decay, the pQCD prediction for the direct CP asymmetry is  $\mathcal{A}_{CP}^{dir}(\bar{B}_s \rightarrow K^+\pi^-) = 0.26 \pm 0.06$ , which agrees very well with the only measured value available currently.

PACS numbers: 13.25.Hw, 12.38.Bx, 14.40.Nd

---

<sup>\*</sup> xiaozhenjun@njnu.edu.cn

## I. INTRODUCTION

The two-body charmless hadronic decays of  $B$  or  $B_s$  meson are the good place to test the Standard Model (SM) and look for the signal of new physics beyond the SM. Since 1999, more than  $10^9$  events of  $B\bar{B}$  pair production and decay have been collected and studied in the B factory experiments. In the Large Hadron Collider (LHC) experiments (ATLAS, CMS and LHC-b), besides those light  $B_{u,d}$  mesons, a huge number of heavier  $B_s$  meson production and decay events will be collected [1]. The study about the charmless decays of  $B_s$  meson is therefore becoming more interesting then ever before.

By employing the generalized factorization approach[2, 3] or the QCD factorization (QCDF) approach [4], about 40  $B_s \rightarrow M_2 M_3$  ( $M_i$  stands for the light pseudo-scalar or vector mesons ) decay modes have been studied, for example, in the framework of SM [5, 6] or in some new physics models beyond the SM [7]. Many  $B_s$  meson decays have also been calculated, on the other hand, by employing the perturbative QCD (pQCD) factorization approach at leading order [8, 9, 10].

Very recently, some next-to-leading order (NLO) contributions to some  $B \rightarrow M_2 M_3$  decays have been calculated by employing the pQCD approach[11, 12, 13]. One can see from those studies that the NLO contributions can change significantly the leading order (LO) pQCD predictions for some decay modes. It is therefore necessary to calculate the NLO contributions to those two-body charmless  $B_s$  meson decays, in order to improve the reliability of the theoretical predictions.

we here focus on the calculations of NLO contributions to  $B_s \rightarrow PP$  decays ( $P = \pi, K, \eta^{(\prime)}$ ) in the pQCD approach. The NLO contributions considered here include: QCD vertex corrections, the quark-loops and the chromo-magnetic penguins. We expect that they are the major part of the full NLO contributions in pQCD approach [11]. The remaining NLO contributions in pQCD approach, such as those from the factorizable emission diagrams, hard-spectator and annihilation diagrams as illustrated in Figs. 5-7 in Ref. [13], have not been calculated at present and should be studied as soon as possible.

This paper is organized as follows. In Sec. II, we give a brief review about the pQCD factorization approach. In Sec. III, we calculate analytically the relevant Feynman diagrams and present the various decay amplitudes for the studied decay modes in the leading-order. In Sec. IV, the NLO contributions from the vertex corrections, the quark loops and the chromo-magnetic penguin amplitudes are evaluated. We calculate and show the pQCD predictions for the branching ratios and CP violating asymmetries of  $B_s \rightarrow PP$  decays in Sec. V. The summary and some discussions are included in the final section.

## II. THEORETICAL FRAMEWORK

### A. Decay amplitude in pQCD

In the pQCD approach, the decay amplitude is separated into soft ( $\Phi_{M_i}$ ), hard ( $H(k_i, t)$ ), and harder ( $C(M_W)$ ) dynamics characterized by different energy scales ( $\Lambda_{QCD}, t, m_b, M_W$ ) [14]. The decay amplitude  $\mathcal{A}(B \rightarrow M_2 M_3)$  can be written conceptually as the convolution,

$$\mathcal{A}(B \rightarrow M_2 M_3) \sim \int d^4 k_1 d^4 k_2 d^4 k_3 \text{Tr} [C(t)\Phi_B(k_1)\Phi_{M_2}(k_2)\Phi_{M_3}(k_3)H(k_1, k_2, k_3, t)], \quad (1)$$

where  $k_i$ 's are momenta of light quarks included in each meson, and  $\text{Tr}$  denotes the trace over Dirac and color indices.  $C(t)$  is the Wilson coefficient evaluated at scale  $t$ . The hard function  $H(k_1, k_2, k_3, t)$  describes the four quark operator and the spectator quark connected by a hard gluon whose  $q^2$  is in the order of  $\Lambda M_B$ , and can be perturbatively calculated. The function  $\Phi_{M_i}$  is the wave function which describes hadronization of the quark and anti-quark in the meson  $M_i$ . While the hard kernel  $H$  depends on the processes considered, the wave function  $\Phi_{M_i}$  is independent of the specific processes. Using the wave functions determined from other well measured processes, one can make quantitative predictions here.

Since the  $b$  quark inside the  $B$  meson is rather heavy, we consider the  $B$  meson at rest for simplicity. Using the light-cone coordinates, we define the emitted meson  $M_2$  moving along the direction of  $n = (1, 0, \mathbf{0}_T)$  and the recoiled meson  $M_3$  the direction of  $v = (0, 1, \mathbf{0}_T)$ . Here we also use  $x_i$  to denote the momentum fraction of anti-quark in each meson:

$$\begin{aligned} P_{B_s} &= \frac{M_B}{\sqrt{2}}(1, 1, \mathbf{0}_T), & P_2 &= \frac{M_{B_s}}{\sqrt{2}}(1, 0, \mathbf{0}_T), & P_3 &= \frac{M_{B_s}}{\sqrt{2}}(0, 1, \mathbf{0}_T), \\ k_1 &= (x_1 P_1^+, 0, \mathbf{k}_{1T}), & k_2 &= (x_2 P_2^+, 0, \mathbf{k}_{2T}), & k_3 &= (0, x_3 P_3^-, \mathbf{k}_{3T}). \end{aligned} \quad (2)$$

Then, the integration over  $k_1^-$ ,  $k_2^-$ , and  $k_3^+$  in eq.(1) will lead to

$$\begin{aligned} \mathcal{A} &\sim \int dx_1 dx_2 dx_3 b_1 db_1 b_2 db_2 b_3 db_3 \\ &\cdot \text{Tr} [C(t) \Phi_B(x_1, b_1) \Phi_{M_2}(x_2, b_2) \Phi_{M_3}(x_3, b_3) H(x_i, b_i, t) S_t(x_i) e^{-S(t)}], \end{aligned} \quad (3)$$

where  $b_i$  is the conjugate space coordinate of  $k_{iT}$ . The large logarithms ( $\ln m_W/t$ ) coming from QCD radiative corrections to four quark operators are included in the Wilson coefficients  $C(t)$ . The large double logarithms ( $\ln^2 x_i$ ) on the longitudinal direction are summed by the threshold resummation, and they lead to  $S_t(x_i)$  which smears the end-point singularities on  $x_i$ . The last term,  $e^{-S(t)}$ , is the Sudakov form factor which suppresses the soft dynamics effectively [14].

## B. Effective Hamiltonian and Wilson coefficients

For the studied  $B_s \rightarrow PP$  decays, the weak effective Hamiltonian  $H_{eff}$  for  $b \rightarrow s$  transition can be written as [15]

$$\mathcal{H}_{eff} = \frac{G_F}{\sqrt{2}} \sum_{q=u,c} V_{qb} V_{qs}^* \left\{ [C_1(\mu) O_1^q(\mu) + C_2(\mu) O_2^q(\mu)] + \sum_{i=3}^{10} C_i(\mu) O_i(\mu) \right\}. \quad (4)$$

where  $G_F = 1.16639 \times 10^{-5} GeV^{-2}$  is the Fermi constant, and  $V_{ij}$  is the Cabbibo-Kobayashi-Maskawa (CKM) matrix element,  $C_i(\mu)$  are the Wilson coefficients evaluated at the renormalization scale  $\mu$  and  $O_i(\mu)$  are the four-fermion operators. For the case of  $b \rightarrow d$  transition, simply makes a replacement of  $s$  by  $d$  in Eq. (4) and in the expressions of  $O_i(\mu)$  operators, which can be found easily for example in Ref.[15].

In PQCD approach, the energy scale “ $t$ ” is chosen as the largest energy scale in the hard kernel  $H(x_i, b_i, t)$  of a given Feynman diagram, in order to suppress the higher order

corrections and improve the reliability of the perturbative calculation. Here, the scale “ $t$ ” may be larger or smaller than the  $m_b$  scale. In the range of  $t \geq m_b$ , the number of active quarks is  $N_f = 5$ , and the renormalization group (RG) running of the Wilson coefficients  $C_i(t)$  and LO and NLO level can be written as [15].

$$\begin{aligned} C_i(t)^{LO} &= U(t, M_W)_{ij}^{(0)} C_j(M_W)^{LO}, \\ C_i(t)^{NLO} &= U(t, M_W, \alpha)_{ij} C_j(M_W)^{NLO}. \end{aligned} \quad (5)$$

The explicit expressions of  $C_i^{LO, NLO}(M_W)$ , the RG evolution matrix  $U(t, M_W)^{(0)}$  and  $U(t, M_W, \alpha)$  can be found easily, for example, in Refs. [15].

In the range of  $\mu_0 \leq t < m_b$ , the number of active quarks is  $N_f = 4$ , and we have similarly

$$\begin{aligned} C_i(t)^{LO} &= U(t, m_b)_{ij}^{(0)} C_j(m_b)^{LO}, \\ C_i(t)^{NLO} &= U(t, m_b, \alpha)_{ij} C_j(m_b)^{NLO}. \end{aligned} \quad (6)$$

According to the analysis in Ref. [13], we believe that it is reasonable to choose  $\mu_0 = 1.0$  GeV as the lower cut-off of the hard scale  $t$ , which is also close to the hard-collinear scale  $\sqrt{\Lambda m_B} \sim 1.3$  GeV in SCET [16]. In the numerical integrations we will fix the values  $C_i(t)$  at  $C_i(1.0)$  whenever the scale  $t$  runs below the scale  $\mu_0 = 1.0$  GeV.

### C. Wave functions

As usual, we treat the  $B$  meson as a very good heavy-light system, and consider only the contribution of Lorentz structure

$$\Phi_{B_s} = \frac{1}{\sqrt{2N_c}} (\not{P}_{B_s} + m_{B_s}) \gamma_5 \phi_{B_s}(\mathbf{k}_1), \quad (7)$$

with

$$\phi_{B_s}(x, b) = N_{B_s} x^2 (1-x)^2 \exp \left[ -\frac{M_{B_s}^2 x^2}{2\omega_b^2} - \frac{1}{2}(\omega_b b)^2 \right], \quad (8)$$

where  $\omega_b$  is a free parameter and we take  $\omega_b = 0.5 \pm 0.05$  GeV for  $B_s$  meson. For a given  $\omega_b$ , the normalization factor  $N_{B_s}$  can be determined through the normalization condition

$$\int \frac{d^4 k_1}{(2\pi)^4} \phi_{B_s}(\mathbf{k}_1) = \frac{f_{B_s}}{2\sqrt{6}}, \quad (9)$$

with  $f_{B_s} = 230$  MeV.

For the  $\eta - \eta'$  system, we employ the quark-flavor mixing scheme: the physical states  $\eta$  and  $\eta'$  are related to the flavor states  $\eta_q = (u\bar{u} + d\bar{d})/\sqrt{2}$  and  $\eta_s = s\bar{s}$  through a single mixing angle  $\phi$ ,

$$\begin{pmatrix} \eta \\ \eta' \end{pmatrix} = \begin{pmatrix} \cos \phi & -\sin \phi \\ \sin \phi & \cos \phi \end{pmatrix} \begin{pmatrix} \eta_q \\ \eta_s \end{pmatrix}. \quad (10)$$

The relation between the decay constants  $(f_\eta^q, f_\eta^s, f_{\eta'}^q, f_{\eta'}^s)$  and  $(f_q, f_s, \phi)$ , the chiral enhancement  $m_0^q$  and  $m_0^s$  associated with the two-parton twist-3  $\eta_q$  and  $\eta_s$  meson distribution amplitudes (DA's) have been defined in Ref.[11]. The three relevant input parameters  $f_q, f_s$  and  $\phi$  have been extracted from the data of the relevant exclusive processes [17]:

$$f_q = (1.07 \pm 0.02)f_\pi, \quad f_s = (1.34 \pm 0.06)f_\pi, \quad \phi = 39.3^\circ \pm 1.0^\circ, \quad (11)$$

with  $f_\pi = 130$  MeV.

For the light pseudo-scalar mesons  $\pi$  and  $K$ , as well as  $\eta_q$  and  $\eta_s$ , their wave functions are the same in form and can be defined as [18]

$$\Phi(P, x, \zeta) \equiv \frac{1}{\sqrt{2N_C}} \gamma_5 [\not{P}\phi^A(x) + m_0\phi^P(x) + \zeta m_0(\not{p}\not{\psi} - 1)\phi_P^T(x)], \quad (12)$$

where  $P$  and  $x$  are the momentum of the light meson and the momentum fraction of the quark (or anti-quark) inside the meson, respectively. When the momentum fraction of the quark (anti-quark) is set to be  $x$ , the parameter  $\zeta$  should be chosen as  $+1$  ( $-1$ ).

The expressions of the relevant DA's of the meson  $M = (\pi, K, \eta_q, \eta_s)$  are the following [18]:

$$\phi_M^A(x) = \frac{3f_M}{\sqrt{6}} x(1-x) \left[ 1 + a_1^M C_1^{3/2}(t) + a_2^M C_2^{3/2}(t) \right], \quad (13)$$

$$\phi_M^P(x) = \frac{f_M}{2\sqrt{6}} \left[ 1 + \left( 30\eta_3 - \frac{5}{2}\rho_M^2 \right) C_2^{1/2}(t) \right], \quad (14)$$

$$\phi_M^T(x) = \frac{f_M(1-2x)}{2\sqrt{6}} \left[ 1 + 6 \left( 5\eta_3 - \frac{1}{2}\eta_3\omega_3 - \frac{7}{20}\rho_M^2 - \frac{3}{5}\rho_M^2 a_2^M \right) (1 - 10x + 10x^2) \right], \quad (15)$$

with the mass ratio  $\rho_M = (m_\pi/m_0^\pi, m_K/m_0^K, m_{qq}/m_0^q, m_{ss}/m_0^s)$  for  $M = (\pi, K, \eta_q, \eta_s)$  respectively [11, 13]. The Gegenbauer moments  $a_i^M$  have been chosen as [10]:

$$\begin{aligned} a_1^\pi &= a_1^{\eta_q, \eta_s} = 0, & a_2^\pi &= a_2^{\eta_q, \eta_s} = 0.44, \\ a_1^K &= 0.17, & a_2^K &= 0.20. \end{aligned} \quad (16)$$

The values of other parameters are  $\eta_3 = 0.015$  and  $\omega = -3.0$ . At last the Gegenbauer polynomials  $C_n^\nu(t)$  in Eqs. (13-15) are defined as:

$$C_1^{3/2}(t) = 3t, \quad C_2^{1/2}(t) = \frac{1}{2}(3t^2 - 1), \quad C_2^{3/2}(t) = \frac{3}{2}(5t^2 - 1), \quad (17)$$

with  $t = 2x - 1$ . Like Ref. [10], we here also drop the terms proportional to  $C_4^{1/2, 3/2}(t)$  in the LCDA's for  $\phi_\pi^A$ ,  $\phi_\pi^P$ , and  $\phi_\pi^T$ .

There are many studies about the distribution amplitudes of light mesons and the relevant Gegenbauer moments [18]. In recent years, the light-cone distribution amplitudes have been updated continually[19]. The inclusion of higher order terms and the variations of the Gegenbauer moments do affect the theoretical predictions for the branching ratios and CP-violating asymmetries of the considered decays, but the resultant changes of theoretical predictions are indeed not significant, according to the analysis in Ref. [10].

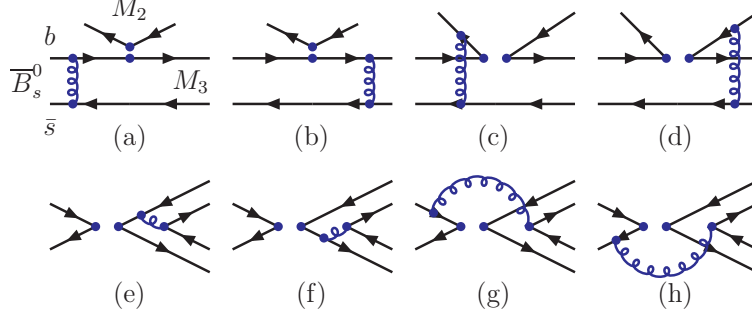


FIG. 1: Feynman diagrams which may contribute at leading order to  $B_s^0 \rightarrow PP$  decays.

### III. DECAY AMPLITUDES AT LEADING ORDER

The thirteen  $B_s^0 \rightarrow PP$  decays ( $P = \pi, K, \eta, \eta'$ ) have been studied previously in Ref. [10] by employing the pQCD factorization approach at leading order. The decay amplitudes as presented in Ref.[10] are confirmed by our recalculation. In this paper, we focus on the calculations of some NLO contributions to these decays in the pQCD factorization approach.

At the leading order, the relevant Feynman diagrams which may contribute to the  $B_s^0 \rightarrow PP$  decays are illustrated in Fig. 1. For the sake of completeness, however, we firstly show the relevant LO decay amplitudes in this section based on our own analytical calculations.

For  $\bar{B}_s^0 \rightarrow K^0 \eta^{(\prime)}$  decays, the LO decay amplitudes are

$$\mathcal{A}(\bar{B}_s^0 \rightarrow K^0 \eta) = \mathcal{A}(\bar{B}_s^0 \rightarrow K^0 \eta_q) \cos(\phi) - \mathcal{A}(\bar{B}_s^0 \rightarrow K^0 \eta_s) \sin(\phi), \quad (18)$$

$$\mathcal{A}(\bar{B}_s^0 \rightarrow K^0 \eta') = \mathcal{A}(\bar{B}_s^0 \rightarrow K^0 \eta_q) \sin(\phi) + \mathcal{A}(\bar{B}_s^0 \rightarrow K^0 \eta_s) \cos(\phi), \quad (19)$$

with

$$\begin{aligned} \sqrt{2}\mathcal{A}(\bar{B}_s^0 \rightarrow K^0 \eta_q) = & \xi_u (f_q F_{eK} a_2 + M_{eK} C_2) \\ & - \xi_t \left\{ f_q F_{eK} \left( 2a_3 + a_4 - 2a_5 - \frac{1}{2}a_7 + \frac{1}{2}a_9 - \frac{1}{2}a_{10} \right) \right. \\ & + M_{eK} \left( C_3 + 2C_4 + 2C_6 + \frac{1}{2}C_8 - \frac{1}{2}C_9 + \frac{1}{2}C_{10} \right) \\ & + f_{B_s} F_{aK} \left( a_4 - \frac{1}{2}a_{10} \right) + (f_{B_s} F_{aK}^{P_2} + f_q F_{eK}^{P_2}) \left( a_6 - \frac{1}{2}a_8 \right) \\ & \left. + M_{aK} \left( C_3 - \frac{1}{2}C_9 \right) + M_{aK}^{P_1} \left( C_5 - \frac{1}{2}C_7 \right) \right\}, \quad (20) \end{aligned}$$

$$\begin{aligned}
\mathcal{A}(\bar{B}_s^0 \rightarrow K^0 \eta_s) = & -\xi_t \left\{ f_s F_{eK} \left( a_3 - a_5 + \frac{1}{2}a_7 - \frac{1}{2}a_9 \right) \right. \\
& + (f_K F_{e\eta_s} + f_{B_s} F_{aK}) \left( a_4 - \frac{1}{2}a_{10} \right) \\
& + (f_K F_{e\eta_s}^{P_2} + f_{B_s} F_{aK}^{P_2}) \left( a_6 - \frac{1}{2}a_8 \right) + M_{eK} \left( C_4 + C_6 - \frac{1}{2}C_8 - \frac{1}{2}C_{10} \right) \\
& \left. + (M_{e\eta_s} + M_{aK}) \left( C_3 - \frac{1}{2}C_9 \right) + (M_{e\eta_s}^{P_1} + M_{aK}^{P_1}) \left( C_5 - \frac{1}{2}C_7 \right) \right\}, \quad (21)
\end{aligned}$$

where  $\xi_u = V_{ub}V_{ud}^*$ ,  $\xi_t = V_{tb}V_{td}^*$ .

For  $\bar{B}_s^0 \rightarrow \pi^0 \eta^{(\prime)}$  decays, the LO decay amplitudes are

$$\mathcal{A}(\bar{B}_s^0 \rightarrow \pi^0 \eta) = \mathcal{A}(\bar{B}_s^0 \rightarrow \pi^0 \eta_q) \cos(\phi) - \mathcal{A}(\bar{B}_s^0 \rightarrow \pi^0 \eta_s) \sin(\phi), \quad (22)$$

$$\mathcal{A}(\bar{B}_s^0 \rightarrow \pi^0 \eta') = \mathcal{A}(\bar{B}_s^0 \rightarrow \pi^0 \eta_q) \sin(\phi) + \mathcal{A}(\bar{B}_s^0 \rightarrow \pi^0 \eta_s) \cos(\phi), \quad (23)$$

with

$$\begin{aligned}
\mathcal{A}(\bar{B}_s^0 \rightarrow \pi^0 \eta_q) = & \xi'_u (f_{B_s} F_{a\eta_n} a_2 + M_{a\eta_n} C_2) \\
& - \frac{3}{2} \xi'_t [f_{B_s} F_{a\eta_n} (a_7 + a_9) + M_{a\eta_n} C_{10} + M_{a\eta_n}^{P_2} C_8], \quad (24)
\end{aligned}$$

$$\begin{aligned}
\mathcal{A}(\bar{B}_s^0 \rightarrow \pi^0 \eta_s) = & \xi'_u (f_\pi F_{e\eta_s} a_2 + M_{e\eta_s} C_2) \\
& - \frac{3}{2} \xi'_t [f_\pi F_{e\eta_s} (a_9 - a_7) + M_{a\eta_s} (C_8 + C_{10})], \quad (25)
\end{aligned}$$

where  $\xi'_u = V_{ub}V_{us}^*$ ,  $\xi'_t = V_{tb}V_{ts}^*$ .

For  $\bar{B}_s^0 \rightarrow \eta\eta, \eta\eta', \eta'\eta'$  decays, the LO decay amplitudes are

$$\begin{aligned}
\sqrt{2}\mathcal{A}(\bar{B}_s^0 \rightarrow \eta\eta) = & \cos^2(\phi)\mathcal{A}(\bar{B}_s^0 \rightarrow \eta_q\eta_q) - \sin(2\phi)\mathcal{A}(\bar{B}_s^0 \rightarrow \eta_q\eta_s) \\
& + \sin^2(\phi)\mathcal{A}(\bar{B}_s^0 \rightarrow \eta_s\eta_s), \quad (26)
\end{aligned}$$

$$\begin{aligned}
\mathcal{A}(\bar{B}_s^0 \rightarrow \eta\eta') = & [\mathcal{A}(\bar{B}_s^0 \rightarrow \eta_q\eta_q) - \mathcal{A}(\bar{B}_s^0 \rightarrow \eta_s\eta_s)] \cos(\phi) \sin(\phi) \\
& + \cos(2\phi)\mathcal{A}(\bar{B}_s^0 \rightarrow \eta_q\eta_s), \quad (27)
\end{aligned}$$

$$\begin{aligned}
\sqrt{2}\mathcal{A}(\bar{B}_s^0 \rightarrow \eta'\eta') = & \sin^2(\phi)\mathcal{A}(\bar{B}_s^0 \rightarrow \eta_q\eta_q) + \sin(2\phi)\mathcal{A}(\bar{B}_s^0 \rightarrow \eta_q\eta_s) \\
& + \cos^2(\phi)\mathcal{A}(\bar{B}_s^0 \rightarrow \eta_s\eta_s). \quad (28)
\end{aligned}$$

with

$$\mathcal{A}(\bar{B}_s^0 \rightarrow \eta_q \eta_q) = \xi'_u M_{a\eta_n} C_2 - \xi'_t M_{a\eta_n} \left( 2C_4 + 2C_6 + \frac{1}{2}C_8 + \frac{1}{2}C_{10} \right), \quad (29)$$

$$\begin{aligned} \sqrt{2}\mathcal{A}(\bar{B}_s^0 \rightarrow \eta_q \eta_s) &= \xi'_u (f_n F_{e\eta_s} a_2 + M_{e\eta_s} C_2) - \xi'_t \left[ f_n F_{e\eta_s} \left( 2a_3 - 2a_5 - \frac{1}{2}a_7 + \frac{1}{2}a_9 \right) \right. \\ &\quad \left. + M_{a\eta_s} \left( 2C_4 + 2C_6 + \frac{1}{2}C_8 + \frac{1}{2}C_{10} \right) \right], \end{aligned} \quad (30)$$

$$\begin{aligned} \mathcal{A}(\bar{B}_s^0 \rightarrow \eta_s \eta_s) &= -2\xi'_t \left[ f_s F_{e\eta_s} \left( a_3 + a_4 - a_5 + \frac{1}{2}a_7 - \frac{1}{2}a_9 - \frac{1}{2}a_{10} \right) \right. \\ &\quad \left. + (f_s F_{e\eta_s}^{P_2} + f_{B_s} F_{a\eta_s}^{P_2}) \left( a_6 - \frac{1}{2}a_8 \right) \right. \\ &\quad \left. + (M_{e\eta_s} + M_{a\eta_s}) \left( C_3 + C_4 + C_6 - \frac{1}{2}C_8 - \frac{1}{2}C_9 - \frac{1}{2}C_{10} \right) \right]. \end{aligned} \quad (31)$$

For  $\bar{B}_s^0 \rightarrow K^+ \pi^-$ ,  $K^0 \pi^0$ ,  $K^+ K^-$  and  $\bar{K}^0 K^0$  decays, the LO decay amplitudes are

$$\begin{aligned} \mathcal{A}(K^+ \pi^-) &= \xi_u (f_\pi F_{eK} a_1 + M_{eK} C_1) - \xi_t \left\{ f_\pi F_{eK} (a_4 + a_{10}) + f_\pi F_{eK}^{P_2} (a_6 + a_8) \right. \\ &\quad \left. + M_{eK} (C_3 + C_9) + f_{B_s} F_{aK} \left( a_4 - \frac{1}{2}a_{10} \right) + f_{B_s} F_{aK}^{P_2} \left( a_6 - \frac{1}{2}a_8 \right) \right. \\ &\quad \left. + M_{aK} \left( C_3 - \frac{1}{2}C_9 \right) + M_{aK}^{P_1} \left( C_5 - \frac{1}{2}C_7 \right) \right\}, \end{aligned} \quad (32)$$

$$\begin{aligned} \sqrt{2}\mathcal{A}(K^0 \pi^0) &= \xi_u (f_\pi F_{eK} a_2 + M_{eK} C_2) - \xi_t \left\{ f_\pi F_{eK} \left( -a_4 - \frac{3}{2}a_7 + \frac{3}{2}a_9 + \frac{1}{2}a_{10} \right) \right. \\ &\quad \left. - (f_\pi F_{ek}^{P_2} + f_{B_s} F_{aK}^{P_2}) \left( a_6 - \frac{1}{2}a_8 \right) + M_{ek} \left( -C_3 + \frac{3}{2}C_8 + \frac{1}{2}C_9 + \frac{3}{2}C_{10} \right) \right. \\ &\quad \left. - f_{B_s} F_{ak} \left( a_4 - \frac{1}{2}a_{10} \right) - M_{ak} \left( C_3 - \frac{1}{2}C_9 \right) - M_{aK}^{P_1} \left( [C_5 - \frac{1}{2}C_7] \right) \right\}, \end{aligned} \quad (33)$$

$$\begin{aligned} \mathcal{A}(K^+ K^-) &= \xi'_u (f_k F_{ek} a_1 + M_{ek} C_1 + M_{ak} C_2) \\ &\quad - \xi'_t \left\{ f_k F_{ek} (a_4 + a_{10}) + f_k F_{ek}^{P_2} (a_6 + a_8) \right. \\ &\quad \left. + M_{ek} (C_3 + C_9) + M_{ek}^{P_1} (C_5 + C_7) + f_{B_s} F_{ak}^{P_2} \left( a_6 - \frac{1}{2}a_8 \right) \right. \\ &\quad \left. + M_{ak} \left( C_3 + C_4 - \frac{1}{2}C_9 - \frac{1}{2}C_{10} \right) + M_{ak}^{P_1} \left( C_5 - \frac{1}{2}C_7 \right) \right. \\ &\quad \left. M_{ak}^{P_2} \left( C_6 - \frac{1}{2}C_8 \right) + [M_{ak} (C_4 + C_{10}) + M_{ak}^{P_2} (C_6 + C_8)]_{K^+ \leftrightarrow K^-} \right\}, \end{aligned} \quad (34)$$



$$\begin{aligned}
\mathcal{A}(\bar{K}_0 K_0) = & -\xi'_t \left\{ f_k F_{ek} \left( a_4 - \frac{1}{2} a_{10} \right) + (f_k F_{ek}^{P_2} + f_{B_s} F_{ak}^{P_2}) \left( a_6 - \frac{1}{2} a_8 \right) \right. \\
& + M_{ek} \left( C_3 - \frac{1}{2} C_9 \right) + (M_{ek}^{P_1} + M_{ak}^{P_1}) \left( C_5 - \frac{1}{2} C_7 \right) \\
& + M_{ak} \left( C_3 + C_4 - \frac{1}{2} C_9 - \frac{1}{2} C_{10} \right) \\
& \left. + M_{ak} \left( C_4 - \frac{1}{2} C_{10} \right)_{K^0 \leftrightarrow \bar{K}^0} + \left[ M_{ak}^{P_2} \left( C_6 - \frac{1}{2} C_8 \right) + [K^0 \leftrightarrow \bar{K}^0] \right] \right\}. \quad (35)
\end{aligned}$$

The  $\bar{B}_s^0 \rightarrow \pi^+ \pi^-$  and  $\bar{B}_s^0 \rightarrow \pi^0 \pi^0$  decays are pure annihilation processes, and the LO decay amplitudes can be written as:

$$\begin{aligned}
\mathcal{A}(\bar{B}_s^0 \rightarrow \pi^+ \pi^-) = & \sqrt{2} \mathcal{A}(\bar{B}_s^0 \rightarrow \pi^0 \pi^0) \\
= & \xi'_u M_{a\pi} C_2 - \xi'_t \left[ M_{a\pi} \left( 2C_4 + \frac{1}{2} C_{10} \right) + M_{a\pi}^{P_2} \left( 2C_6 + \frac{1}{2} C_8 \right) \right]. \quad (36)
\end{aligned}$$

The individual decay amplitudes, such as  $F_{eK}, F_{e\eta_s}, etc.$ , appeared in Eqs. (18-31), are obtained by evaluating the corresponding Feynman diagrams analytically. For the  $B_s \rightarrow M_3$  transitions, where the meson  $M_3$  absorbed the spectator  $\bar{s}$  quark, the corresponding decay amplitudes can be written as

$$\begin{aligned}
F_{eM_3} = & 8\pi C_F M_{B_s}^4 \int_0^1 dx_1 dx_3 \int_0^\infty b_1 db_1 b_3 db_3 \phi_{B_s}(x_1, b_1) \\
& \cdot \left\{ [(1+x_3)\phi_3^A(x_3) + r_3(1-2x_3)(\phi_3^P(x_3) + \phi_3^T(x_3))] \right. \\
& \cdot \alpha_s(t_e^1) h_e(x_1, x_3, b_1, b_3) \exp[-S_{ab}(t_e^1)] \\
& \left. + 2r_3 \phi_3^P(x_3) \cdot \alpha_s(t_e^2) h_e(x_3, x_1, b_3, b_1) \exp[-S_{ab}(t_e^2)] \right\}, \quad (37)
\end{aligned}$$

$$\begin{aligned}
F_{eM_3}^{P_2} = & 16\pi C_F M_{B_s}^4 r_2 \int_0^1 dx_1 dx_3 \int_0^\infty b_1 db_1 b_3 db_3 \phi_{B_s}(x_1, b_1) \\
& \cdot \left\{ [\phi_3^A(x_3) + r_3(2+x_3)\phi_3^P(x_3) - r_3 x_3 \phi_3^T(x_3)] \right. \\
& \cdot \alpha_s(t_e^1) h_e(x_1, x_3, b_1, b_3) \exp[-S_{ab}(t_e^1)] \\
& \left. + 2r_3 \phi_3^P(x_3) \alpha_s(t_e^2) h_e(x_3, x_1, b_3, b_1) \exp[-S_{ab}(t_e^2)] \right\}, \quad (38)
\end{aligned}$$

$$\begin{aligned}
M_{eM_3} = & \frac{32}{\sqrt{6}} \pi C_F M_{B_s}^4 \int_0^1 dx_1 dx_2 dx_3 \int_0^\infty b_1 db_1 b_2 db_2 \phi_{B_s}(x_1, b_1) \phi_2^A(x_2) \\
& \cdot \left\{ [(1-x_2)\phi_3^A(x_3) - r_3 x_3 (\phi_3^P(x_3) - \phi_3^T(x_3))] \right. \\
& \cdot \alpha_s(t_e^3) h_n(x_1, 1-x_2, x_3, b_1, b_2) \exp[-S_{cd}(t_e^3)] \\
& - [(x_2+x_3)\phi_3^A(x_3) - r_3 x_3 (\phi_3^P(x_3) + \phi_3^T(x_3))] \\
& \left. \cdot \alpha_s(t_e^4) h_n(x_1, x_2, x_3, b_1, b_2) \exp[-S_{cd}(t_e^4)] \right\}, \quad (39)
\end{aligned}$$

$$\begin{aligned}
M_{eM_3}^{P_1} &= \frac{32}{\sqrt{6}} \pi C_F M_{B_s}^4 r_2 \int_0^1 dx_1 dx_2 dx_3 \int_0^\infty b_1 db_1 b_2 db_2 \phi_{B_s}(x_1, b_1) \\
&\cdot \left\{ [(1-x_2)\phi_3^A(x_3) (\phi_2^P(x_2) + \phi_2^T(x_2)) \right. \\
&+ r_3 x_3 (\phi_2^P(x_2) - \phi_2^T(x_2)) (\phi_3^P(x_3) + \phi_3^T(x_3)) \\
&+ r_3(1-x_2) (\phi_2^P(x_2) + \phi_2^T(x_2)) (\phi_3^P(x_3) - \phi_3^T(x_3))] \\
&\cdot \alpha_s(t_e^3) h_n(x_1, 1-x_2, x_3, b_1, b_2) \exp[-S_{cd}(t_e^3)] \\
&+ [x_2 \phi_3^A(x_3) (\phi_2^P(x_2) - \phi_2^T(x_2)) + r_3 x_2 (\phi_2^P(x_2) - \phi_2^T(x_2)) (\phi_3^P(x_3) - \phi_3^T(x_3)) \\
&+ r_3 x_3 (\phi_2^P(x_2) + \phi_2^T(x_2)) (\phi_3^P(x_3) + \phi_3^T(x_3))] \\
&\cdot \alpha_s(t_e^4) h_n(x_1, x_2, x_3, b_1, b_2) \exp[-S_{cd}(t_e^4)] \left. \right\} . \tag{40}
\end{aligned}$$

$$\begin{aligned}
M_{eM_3}^{P_2} &= \frac{32}{\sqrt{6}} \pi C_F M_{B_s}^4 \int_0^1 dx_1 dx_2 dx_3 \int_0^\infty b_1 db_1 b_2 db_2 \phi_{B_s}(x_1, b_1) \phi_2^A(x_2) \\
&\cdot \left\{ [(x_2 - x_3 - 1)\phi_3^A(x_3) + r_3 x_3 (\phi_3^P(x_3) + \phi_3^T(x_3))] \right. \\
&\cdot \alpha_s(t_e^3) h_n(x_1, 1-x_2, x_3, b_1, b_2) \exp[-S_{cd}(t_e^3)] \\
&+ [x_2 \phi_3^A(x_3) + r_3 x_3 (\phi_3^P(x_3) - \phi_3^T(x_3))] \\
&\cdot \alpha_s(t_e^4) h_n(x_1, x_2, x_3, b_1, b_2) \exp[-S_{cd}(t_e^4)] \left. \right\} , \tag{41}
\end{aligned}$$

$$\begin{aligned}
F_{aM_3} &= 8\pi C_F M_{B_s}^4 \int_0^1 dx_2 dx_3 \int_0^\infty b_2 db_2 b_3 db_3 \cdot \left\{ [(x_3 - 1)\phi_2^A(x_2)\phi_3^A(x_3) \right. \\
&- 4r_2 r_3 \phi_2^P(x_2)\phi_3^P(x_3) + 2r_2 r_3 x_3 \phi_2^P(x_2) (\phi_3^P(x_3) - \phi_3^T(x_3))] \\
&\cdot \alpha_s(t_e^5) h_a(x_2, 1-x_3, b_2, b_3) \exp[-S_{ef}(t_e^5)] \\
&+ [x_2 \phi_2^A(x_2)\phi_3^A(x_3) + 2r_2 r_3 (\phi_2^P(x_2) - \phi_2^T(x_2)) \phi_3^P(x_3) \\
&+ 2r_2 r_3 x_2 (\phi_2^P(x_2) + \phi_2^T(x_2)) \phi_3^P(x_3)] \\
&\cdot \alpha_s(t_e^6) h_a(1-x_3, x_2, b_3, b_2) \exp[-S_{ef}(t_e^6)] \left. \right\} , \tag{42}
\end{aligned}$$

$$\begin{aligned}
F_{aM_3}^{P_2} &= 16\pi C_F M_{B_s}^4 \int_0^1 dx_2 dx_3 \int_0^\infty b_2 db_2 b_3 db_3 \\
&\cdot \left\{ [2r_2 \phi_2^P(x_2)\phi_3^A(x_3) + (1-x_3)r_3 \phi_2^A(x_2) (\phi_3^P(x_3) + \phi_3^T(x_3))] \right. \\
&\cdot \alpha_s(t_e^5) h_a(x_2, 1-x_3, b_2, b_3) \exp[-S_{ef}(t_e^5)] \\
&+ [2r_3 \phi_2^A(x_2)\phi_3^P(x_3) + r_2 x_2 (\phi_2^P(x_2) - \phi_2^T(x_2)) \phi_3^A(x_3)] \\
&\cdot \alpha_s(t_e^6) h_a(1-x_3, x_2, b_3, b_2) \exp[-S_{ef}(t_e^6)] \left. \right\} , \tag{43}
\end{aligned}$$

$$\begin{aligned}
M_{aM_3} &= \frac{32}{\sqrt{6}}\pi C_F M_{B_s}^4 \int_0^1 dx_1 dx_2 dx_3 \int_0^\infty b_1 db_1 b_2 db_2 \phi_{B_s}(x_1, b_1) \\
&\cdot \{ [-x_2 \phi_2^A(x_2) \phi_3^A(x_3) - 4r_2 r_3 \phi_2^P(x_2) \phi_3^P(x_3) \\
&+ r_2 r_3 (1-x_2) (\phi_2^P(x_2) + \phi_2^T(x_2)) (\phi_3^P(x_3) - \phi_3^T(x_3)) \\
&+ r_2 r_3 x_3 (\phi_2^P(x_2) - \phi_2^T(x_2)) (\phi_3^P(x_3) + \phi_3^T(x_3))] \\
&\cdot \alpha_s(t_e^7) h_{na}(x_1, x_2, x_3, b_1, b_2) \exp[-S_{gh}(t_e^7)] \\
&+ [(1-x_3) \phi_2^A(x_2) \phi_3^A(x_3) + (1-x_3) r_2 r_3 (\phi_2^P(x_2) + \phi_2^T(x_2)) (\phi_3^P(x_3) - \phi_3^T(x_3)) \\
&+ x_2 r_2 r_3 (\phi_2^P(x_2) - \phi_2^T(x_2)) (\phi_3^P(x_3) + \phi_3^T(x_3))] \\
&\cdot \alpha_s(t_e^8) h'_{na}(x_1, x_2, x_3, b_1, b_2) \exp[-S_{gh}(t_e^8)] \} , \tag{44}
\end{aligned}$$

$$\begin{aligned}
M_{aM_3}^{P_1} &= \frac{32}{\sqrt{6}}\pi C_F M_{B_s}^4 \int_0^1 dx_1 dx_2 dx_3 \int_0^\infty b_1 db_1 b_2 db_2 \phi_{B_s}(x_1, b_1) \\
&\cdot \{ [r_2(2-x_2) (\phi_2^P(x_2) + \phi_2^T(x_2)) \phi_3^A(x_3) + r_3(1+x_3) \phi_2^A(x_2) (\phi_3^P(x_3) - \phi_3^T(x_3))] \\
&\cdot \alpha_s(t_e^7) \exp[-S_{gh}(t_e^7)] h_{na}(x_1, x_2, x_3, b_1, b_2) \\
&+ [r_2 x_2 (\phi_2^P(x_2) + \phi_2^T(x_2)) \phi_3^A(x_3) - (1-x_3) r_3 \phi_2^A(x_2) (\phi_3^P(x_3) - \phi_3^T(x_3))] \\
&\cdot \alpha_s(t_e^8) h'_{na}(x_1, x_2, x_3, b_1, b_2) \exp[-S_{gh}(t_e^8)] \} , \tag{45}
\end{aligned}$$

$$\begin{aligned}
M_{aM_3}^{P_2} &= \frac{32}{\sqrt{6}}\pi C_F M_{B_s}^4 \int_0^1 dx_1 dx_2 dx_3 \int_0^\infty b_1 db_1 b_2 db_2 \phi_{B_s}(x_1, b_1) \\
&\cdot \{ [(x_3-1) \phi_2^A(x_2) \phi_3^A(x_3) - 4r_2 r_3 \phi_2^P(x_2) \phi_3^P(x_3) \\
&+ r_2 r_3 x_3 (\phi_2^P(x_2) + \phi_2^T(x_2)) (\phi_3^P(x_3) - \phi_3^T(x_3)) \\
&+ r_2 r_3 (1-x_2) (\phi_2^P(x_2) - \phi_2^T(x_2)) (\phi_3^P(x_3) + \phi_3^T(x_3))] \\
&\cdot \alpha_s(t_e^7) h_{na}(x_1, x_2, x_3, b_1, b_2) \exp[-S_{gh}(t_e^7)] \\
&+ [x_2 \phi_2^A(x_2) \phi_3^A(x_3) + x_2 r_2 r_3 (\phi_2^P(x_2) + \phi_2^T(x_2)) (\phi_3^P(x_3) - \phi_3^T(x_3)) \\
&+ r_2 r_3 (1-x_3) (\phi_2^P(x_2) - \phi_2^T(x_2)) (\phi_3^P(x_3) + \phi_3^T(x_3))] \\
&\cdot \alpha_s(t_e^8) h'_{na}(x_1, x_2, x_3, b_1, b_2) \exp[-S_{gh}(t_e^8)] \} , \tag{46}
\end{aligned}$$

where  $C_F = 4/3$  is the color-factor,  $r_2 = m_0^{M_2}/M_{B_s}$  and  $r_3 = m_0^{M_3}/M_{B_s}$  with the chiral enhancement factor  $m_0$  for meson  $M_2$  and  $M_3$ . Here  $(F_{eM_3}, F_{eM_3}^{P_2})$  and  $(M_{eM_3}, F_{eM_3}^{P_1, P_2})$  come from the factorizable emission diagrams ( Fig.1a and 1b) and the non-factorizable hard spectator diagrams (Fig.1c and 1d), respectively; and  $(F_{aM_3}, F_{aM_3}^{P_2})$  and  $(M_{aM_3}, F_{aM_3}^{P_1, P_2})$  are obtained by evaluating the factorizable annihilation diagrams ( Fig.1e and 1f) and the non-factorizable annihilation diagrams (Fig.1g and 1h), respectively. The explicit expressions of the hard energy scale  $(t_e^1, t_e^2, \dots, t_e^8)$ , the hard functions  $(h_e, h_n, h_a, h_{na}, h'_{na})$ , the Sudakov factors  $(S_{ab}(t_e), S_{cd}(t_e), S_{ef}(t_e), S_{gh}(t_e))$  can be found in Appendix A.

#### IV. NEXT-TO-LEADING ORDER CONTRIBUTIONS

At next-to-leading order, firstly, the NLO Wilson coefficients  $C_i(M_W)$ , the NLO RG evolution matrix  $U(t, m, \alpha)$  [15], and the  $\alpha_s(t)$  at two-loop level will be employed.

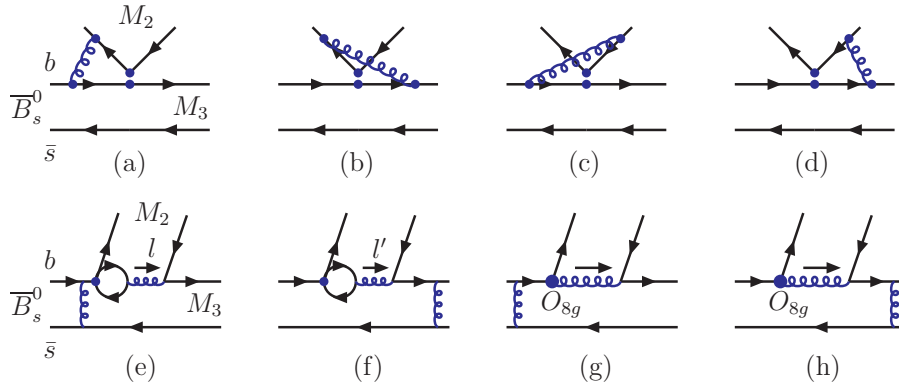


FIG. 2: Feynman diagrams for NLO contributions: the vertex corrections (a-d); the quark-loop (e-f) and the chromo-magnetic penguin contributions (g-h).

Secondly, the NLO hard kernel  $H^{(1)}(\alpha_s^2)$  should be included. All the Feynman diagrams, in other words, which lead to the decay amplitudes proportional to  $\alpha_s^2(t)$ , should be considered. Such Feynman diagrams can be grouped into following classes:

I: The vertex corrections, as illustrated in Figs. 2a-2d, the same set as in the QCDF approach.

II: The NLO contributions from quark-loops, as illustrated in Figs. 2e-2f.

III: The NLO contributions from chromo-magnetic penguins, i.e. the operator  $O_{8g}$ , as illustrated in Figs. 2g-2h. There are totally nine relevant Feynman diagrams as given in Ref. [20], if the Feynman diagrams involving three-gluon vertex are also included. We here show the first two only, and they provide the dominant NLO contributions, according to Ref. [20].

IV: The NLO corrections to the LO emission diagrams(1a,1b), the LO hard-spectator(1c,1d) and the LO annihilation diagrams (1e-1h), as illustrated in Fig. 3. One can draw more than one hundred such Feynman diagrams in total, but we here show representative ones only.

At present, the calculations for the vertex corrections, the quark-loops and chromo-magnetic penguins have been available and will be considered here. We expect that they are the major part of the full NLO contributions in pQCD approach [11]. For the Feynman diagrams as shown in Fig. 3, however, the analytical calculations have not been completed yet. Of course, these Feynman diagrams should be calculated as soon as possible, in order to improve the reliability of the pQCD predictions.

### A. Vertex corrections, quark-loops and chromo-magnetic penguins

The vertex corrections to the factorizable emission diagrams, as illustrated by Figs. 2a-2d, have been calculated years ago in the QCD factorization approach[4, 6]. For  $B_s \rightarrow PP$  decays, the vertex corrections can be calculated without considering the transverse

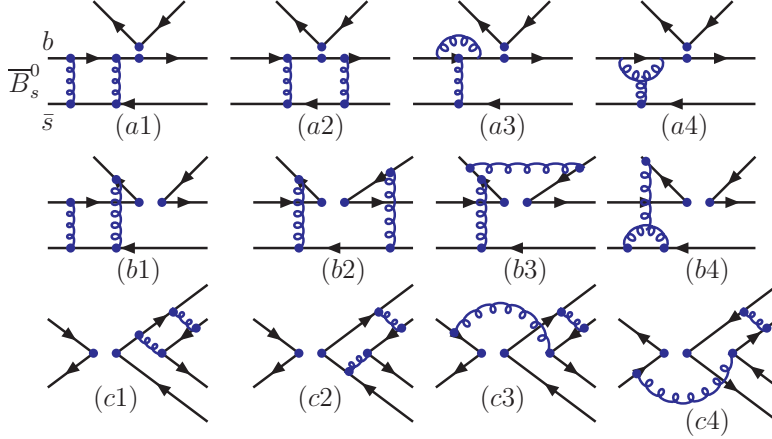


FIG. 3: The typical Feynman diagrams, which provide NLO contributions to the factorizable emission amplitudes (a1-a4), the hard-spectator amplitude (b1-b4), and the annihilation amplitudes (c1-c4)

momentum effects of the quark at the end-point [11], one can use the vertex corrections as given in Ref. [6] directly. The vertex corrections can then be absorbed into the redefinition of the Wilson coefficients  $a_i(\mu)$  by adding a vertex-function  $V_i(M)$  to them [4, 6]

$$\begin{aligned}
a_i(\mu) &\rightarrow a_i(\mu) + \frac{\alpha_s(\mu)}{4\pi} C_F \frac{C_i(\mu)}{3} V_i(M), \quad \text{for } i = 1, 2; \\
a_j(\mu) &\rightarrow a_j(\mu) + \frac{\alpha_s(\mu)}{4\pi} C_F \frac{C_{j+1}(\mu)}{3} V_j(M), \quad \text{for } j = 3, 5, 7, 9, \\
a_j(\mu) &\rightarrow a_j(\mu) + \frac{\alpha_s(\mu)}{4\pi} C_F \frac{C_{j-1}(\mu)}{3} V_j(M), \quad \text{for } j = 4, 6, 8, 10,
\end{aligned} \tag{47}$$

where  $M$  is the meson emitted from the weak vertex. When  $M$  is a pseudo-scalar meson, the vertex functions  $V_i(M)$  are given ( in the NDR scheme) in Refs. [6, 11]:

$$V_i(M) = \begin{cases} 12 \ln \frac{m_b}{\mu} - 18 + \frac{2\sqrt{6}}{f_M} \int_0^1 dx \phi_M^A(x) g(x), & \text{for } i = 1 - 4, 9, 10, \\ -12 \ln \frac{m_b}{\mu} + 6 - \frac{2\sqrt{6}}{f_M} \int_0^1 dx \phi_M^A(x) g(1-x), & \text{for } i = 5, 7, \\ -6 + \frac{2\sqrt{6}}{f_M} \int_0^1 dx \phi_M^P(x) h(x), & \text{for } i = 6, 8, \end{cases} \tag{48}$$

where  $f_M$  is the decay constant of the meson  $M$ ;  $\phi_M^A(x)$  and  $\phi_M^P(x)$  are the twist-2 and twist-3 distribution amplitude of the meson  $M$ , respectively. The hard-scattering functions  $g(x)$  and  $h(x)$  in Eq. (48) are:

$$g(x) = 3 \left( \frac{1-2x}{1-x} \ln x - i\pi \right) + \left[ 2Li_2(x) - \ln^2 x + \frac{2 \ln x}{1-x} - (3 + 2i\pi) \ln x - (x \leftrightarrow 1-x) \right], \tag{49}$$

$$h(x) = 2Li_2(x) - \ln^2 x - (1 + 2i\pi) \ln x - (x \leftrightarrow 1-x), \tag{50}$$

where  $\text{Li}_2(x)$  is the dilogarithm function. As shown in Ref. [11], the  $\mu$ -dependence of the Wilson coefficients  $a_i(\mu)$  will be improved generally by the inclusion of the vertex corrections.

The contribution from the so-called ‘‘quark-loops’’ is a kind of penguin correction with the four quark operators insertion, as illustrated by Fig. 2e and 2f. We here include quark-loop amplitude from the operators  $O_{1,2}$  and  $O_{3-6}$  only. The quark loops from  $O_{7-10}$  will be neglected due to their smallness.

For the  $b \rightarrow s$  transition, the effective Hamiltonian  $H_{eff}^{ql}$  which describes the contributions from the quark loops can be written as [11]

$$H_{eff}^{(ql)} = - \sum_{q=u,c,t} \sum_{q'} \frac{G_F}{\sqrt{2}} V_{qb} V_{qs}^* \frac{\alpha_s(\mu)}{2\pi} C^{(q)}(\mu, l^2) (\bar{s} \gamma_\rho (1 - \gamma_5) T^a b) (\bar{q}' \gamma^\rho T^a q'), \quad (51)$$

where  $l^2$  is the invariant mass of the gluon, as illustrated by Fig.2e. The functions  $C^{(q)}(\mu, l^2)$  are given by

$$C^{(q)}(\mu, l^2) = \left[ G^{(q)}(\mu, l^2) - \frac{2}{3} \right] C_2(\mu) \quad (52)$$

for  $q = u, c$  and

$$C^{(t)}(\mu, l^2) = \left[ G^{(s)}(\mu, l^2) - \frac{2}{3} \right] C_3(\mu) + \sum_{q'=u,d,s,c} G^{(q')}(\mu, l^2) [C_4(\mu) + C_6(\mu)] \quad (53)$$

for  $q = t$ . The function  $G^{(q)}(\mu, l^2)$  for the loop of the  $q(q = u, d, s, c)$  quark is given by [11]

$$G^{(q)}(\mu, l^2) = -4 \int_0^1 dx x(1-x) \ln \frac{m_q^2 - x(1-x)l^2}{\mu^2} \quad (54)$$

$m_q$  is the possible quark mass. The explicit expressions of the function  $G^{(q)}(\mu, l^2)$  after the integration can be found, for example, in Ref. [11].

The magnetic penguin is another kind penguin correction induced by the insertion of the operator  $O_{8g}$ , as illustrated by Fig.2g and 2h. The corresponding weak effective Hamiltonian contains the  $b \rightarrow sg$  transition can be written as

$$H_{eff}^{mp} = -\frac{G_F}{\sqrt{2}} V_{tb} V_{ts}^* C_{8g}^{eff} O_{8g}, \quad (55)$$

with the magnetic penguin operator,

$$O_{8g} = \frac{g_s}{8\pi^2} m_b \bar{d}_i \sigma^{\mu\nu} (1 + \gamma_5) T_{ij}^a G_{\mu\nu}^a b_j, \quad (56)$$

where  $i, j$  being the color indices of quarks. The corresponding effective Wilson coefficient  $C_{8g}^{eff} = C_{8g} + C_5$  [11].

It is worth noting that there are totally nine Feynman diagrams involving the  $O_{8g}$  operator as shown in Ref. [20], if the Feynman diagrams involving three-gluon vertex are also included. We here show the first two only, say Fig.2g and 2h, and they provide the dominant NLO contributions from the  $O_{8g}$  operator, according to Ref. [20].

## B. NLO decay amplitudes

Now we are ready to calculate the decay amplitude corresponding to the quark-loops and magnetic penguins. By analytical evaluations, we find two kinds of topological decay amplitudes  $\mathcal{M}_{M_2 M_3}^q$  and  $\mathcal{M}_{M_2 M_3}^g$ , respectively. For  $B \rightarrow \eta_n K^0$  decay, we find

$$\begin{aligned}
\mathcal{M}_{\eta_n K^0}^{(q)} = & -\frac{4}{\sqrt{3}} m_{B_s}^4 C_F^2 \int_0^1 dx_1 dx_2 dx_3 \int_0^\infty b_1 db_1 b_3 db_3 \phi_{B_s}(x_1) \{ [(1+x_3)\phi_{\eta_n}^A(x_2)\phi_K^A(x_3) \\
& + 2r_{\eta_n}\phi_{\eta_n}^P(x_2)\phi_K^A(x_3) + r_K(1-2x_3)\phi_{\eta_n}(x_2) [\phi_K^P(x_3) + \phi_K^T(x_3)] \\
& + 2r_{\eta_n}r_K\phi_{\eta_n}^P(x_2) [(2+x_3)\phi_K^P(x_3) - x_3\phi_K^T(x_3)]] \\
& \cdot \alpha_s^2(t_e^9) h_e(x_1, x_3, b_1, b_3) \exp[-S_{ab}(t_e^9)] C^{(q)}(t_e^9, l^2) \\
& + [2r_K\phi_{\eta_n}^A(x_2)\phi_K^P(x_3) + 4r_{\eta_n}r_K\phi_{\eta_n}^P(x_2)\phi_K^P(x_3)] \\
& \cdot \alpha_s^2(t_e^{10}) h_e(x_3, x_1, b_3, b_1) \exp[-S_{ab}(t_e^{10})] C^{(q)}(t_e^{10}, l^2) \}, \tag{57}
\end{aligned}$$

$$\begin{aligned}
\mathcal{M}_{\eta_n K^0}^{(g)} = & \frac{8m_{B_s}^6 C_F^2}{\sqrt{3}} \int_0^1 dx_1 dx_2 dx_3 \int_0^\infty b_1 db_1 b_2 db_2 b_3 db_3 \phi_{B_s}(x_1) \{ [-(1-x_3)[\phi_K^A(x_3) \\
& + r_K(3\phi_K^P(x_3) + \phi_K^T(x_3)) + r_K x_3(\phi_K^P(x_3) - \phi_K^T(x_3))] \phi_{\eta_n}^A(x_2) - r_{\eta_n} x_2(1+x_3) \\
& \times (3\phi_{\eta_n}^P(x_2) - \phi_{\eta_n}^T(x_2)) \phi_K^A(x_3) - r_{\eta_n} r_K(1-x_3)(3\phi_{\eta_n}^P(x_2) + \phi_{\eta_n}^T(x_2))(\phi_K^P(x_3) \\
& - \phi_K^T(x_3)) - r_{\eta_n} r_K x_2(1-2x_3)(3\phi_{\eta_n}^P(x_2) - \phi_{\eta_n}^T(x_2))(\phi_K^P(x_3) + \phi_K^T(x_3))] \\
& \cdot \alpha_s^2(t_e^9) h_g(x_1, x_2, x_3, b_1, b_2, b_3) \exp[-S_{cd}(t_e^9)] C_{8g}^{eff}(t_e^9) \\
& - [4r_K\phi_{\eta_n}^A(x_2)\phi_K^P(x_3) + 2r_{\eta_n}r_K x_2(3\phi_{\eta_n}^P(x_2) - \phi_{\eta_n}^T(x_2))\phi_K^P(x_3)] \\
& \cdot \alpha_s^2(t_e^{10}) h'_g(x_1, x_2, x_3, b_1, b_2, b_3) \exp[-S_{cd}(t_e^{10})] C_{8g}^{eff}(t_e^{10}) \}. \tag{58}
\end{aligned}$$

$$\begin{aligned}
\mathcal{M}_{K^0 \eta_s}^{(q)} = & -\frac{8m_{B_s}^4 C_F^2}{\sqrt{6}} \int_0^1 dx_1 dx_2 dx_3 \int_0^\infty b_1 db_1 b_3 db_3 \phi_{B_s}(x_1) \{ [(1+x_3)\phi_K^A(x_2)\phi_{\eta_s}^A(x_3) \\
& + 2r_K\phi_K^P(x_2)\phi_{\eta_s}^A(x_3) + r_{\eta_s}(1-2x_3)\phi_K(x_2) [\phi_{\eta_s}^P(x_3) + \phi_{\eta_s}^T(x_3)] \\
& + 2r_K r_{\eta_s} \phi_K^P(x_2) [(2+x_3)\phi_{\eta_s}^P(x_3) - x_3\phi_{\eta_s}^T(x_3)]] \\
& \cdot \alpha_s^2(t_e^9) h_e(x_1, x_3, b_1, b_3) \exp[-S_{ab}(t_e^9)] C^{(q)}(t_e^9, l^2) \\
& + [2r_{\eta_s}\phi_K^A(x_2)\phi_{\eta_s}^P(x_3) + 4r_K r_{\eta_s} \phi_K^P(x_2)\phi_{\eta_s}^P(x_3)] \\
& \cdot \alpha_s^2(t_e^{10}) h_e(x_3, x_1, b_3, b_1) \exp[-S_{ab}(t_e^{10})] C^{(q)}(t_e^{10}, l^2) \}, \tag{59}
\end{aligned}$$

$$\begin{aligned}
\mathcal{M}_{K^0\eta_s}^{(g)} &= 16m_{B_s}^6 \frac{C_F^2}{\sqrt{2N_c}} \int_0^1 dx_1 dx_2 dx_3 \int_0^\infty b_1 db_1 b_2 db_2 b_3 db_3 \phi_{B_s}(x_1) \\
&\cdot \left\{ [-(1-x_3) [2\phi_{\eta_s}^A(x_3) + r_{\eta_s} [3\phi_{\eta_s}^P(x_3) + \phi_{\eta_s}^T(x_3)] \right. \\
&\quad + r_{\eta_s} x_3 (\phi_{\eta_s}^P(x_3) - \phi_{\eta_s}^T(x_3))] \phi_K^A(x_2) \\
&\quad - r_K x_2 (1+x_3) [3\phi_K^P(x_2) - \phi_K^T(x_2)] \phi_{\eta_s}^A(x_3) \\
&\quad - r_K r_{\eta_s} (1-x_3) (3\phi_K^P(x_2) + \phi_K^T(x_2)) (\phi_{\eta_s}^P(x_3) \\
&\quad - \phi_{\eta_s}^T(x_3)) - r_K r_{\eta_s} x_2 (1-2x_3) (3\phi_K^P(x_2) - \phi_K^T(x_2)) (\phi_{\eta_s}^P(x_3) + \phi_{\eta_s}^T(x_3))] \\
&\quad \cdot \alpha_s^2(t_e^9) C_{8g}^{eff}(t_e^9) h_g(x_1, x_2, x_3, b_1, b_2, b_3) \exp[-S_{cd}(t_e^9)] \\
&\quad - [4r_{\eta_s} \phi_K^A(x_2) \phi_{\eta_s}^P(x_3) + 2r_K r_{\eta_s} x_2 (3\phi_K^P(x_2) - \phi_K^T(x_2)) \phi_{\eta_s}^P(x_3)] \\
&\quad \left. \cdot \alpha_s^2(t_e^{10}) h'_g(x_1, x_2, x_3, b_1, b_2, b_3) \exp[-S_{cd}(t_e^{10})] C_{8g}^{eff}(t_e^{10}) \right\}, \tag{60}
\end{aligned}$$

$$\begin{aligned}
\mathcal{M}_{\eta_s\eta_s}^{(q)} &= -16m_{B_s}^4 \frac{C_F^2}{\sqrt{2N_c}} \int_0^1 dx_1 dx_2 dx_3 \int_0^\infty b_1 db_1 b_3 db_3 \phi_{B_s}(x_1) \left\{ [(1+x_3) \phi_{\eta_s}^A(x_2) \phi_{\eta_s}^A(x_3) \right. \\
&\quad + 2r_{\eta_s} \phi_{\eta_s}^P(x_2) \phi_{\eta_s}^A(x_3) + r_{\eta_s} (1-2x_3) \phi_{\eta_s}(x_2) (\phi_{\eta_s}^P(x_3) + \phi_{\eta_s}^T(x_3)) \\
&\quad + 2r_{\eta_s} r_{\eta_s} \phi_{\eta_s}^P(x_2) ((2+x_3) \phi_{\eta_s}^P(x_3) - x_3 \phi_{\eta_s}^T(x_3))] \\
&\quad \cdot \alpha_s^2(t_e^9) h_e(x_1, x_3, b_1, b_3) \exp[-S_{ab}(t_e^9)] C^{(q)}(t_e^9, l^2) \\
&\quad + [2r_{\eta_s} \phi_{\eta_s}^A(x_2) \phi_{\eta_s}^P(x_3) + 4r_{\eta_s} r_{\eta_s} \phi_{\eta_s}^P(x_2) \phi_{\eta_s}^P(x_3)] \\
&\quad \left. \cdot \alpha_s^2(t_e^{10}) h_e(x_3, x_1, b_3, b_1) \exp[-S_{ab}(t_e^{10})] C^{(q)}(t_e^{10}, l^2) \right\}, \tag{61}
\end{aligned}$$

$$\begin{aligned}
\mathcal{M}_{\eta_s\eta_s}^{(g)} &= -32m_{B_s}^6 \frac{C_F^2}{\sqrt{2N_c}} \int_0^1 dx_1 dx_2 dx_3 \int_0^\infty b_1 db_1 b_2 db_2 b_3 db_3 \phi_{B_s}(x_1) \left\{ [(1-x_3) [2\phi_{\eta_s}^A(x_3) \right. \\
&\quad + r_{\eta_s} (3\phi_{\eta_s}^P(x_3) + \phi_{\eta_s}^T(x_3)) + r_{\eta_s} x_3 (\phi_{\eta_s}^P(x_3) - \phi_{\eta_s}^T(x_3))] \phi_{\eta_s}^A(x_2) \\
&\quad - r_{\eta_s} x_2 (1+x_3) (3\phi_{\eta_s}^P(x_2) - \phi_{\eta_s}^T(x_2)) \phi_{\eta_s}^A(x_3) \\
&\quad - r_{\eta_s} r_{\eta_s} (1-x_3) (3\phi_{\eta_s}^P(x_2) + \phi_{\eta_s}^T(x_2)) (\phi_{\eta_s}^P(x_3) - \phi_{\eta_s}^T(x_3)) \\
&\quad - r_{\eta_s} r_{\eta_s} x_2 (1-2x_3) (3\phi_{\eta_s}^P(x_2) - \phi_{\eta_s}^T(x_2)) (\phi_{\eta_s}^P(x_3) + \phi_{\eta_s}^T(x_3))] \\
&\quad \cdot \alpha_s^2(t_e^9) h_g(x_1, x_2, x_3, b_1, b_2, b_3) \exp[-S_{cd}(t_e^9)] C_{8g}^{eff}(t_e^9) \\
&\quad + [4r_{\eta_s} \phi_{\eta_s}^A(x_2) \phi_{\eta_s}^P(x_3) + 2r_{\eta_s} r_{\eta_s} x_2 (3\phi_{\eta_s}^P(x_2) - \phi_{\eta_s}^T(x_2)) \phi_{\eta_s}^P(x_3)] \\
&\quad \left. \cdot \alpha_s^2(t_e^{10}) h'_g(x_1, x_2, x_3, b_1, b_2, b_3) \exp[-S_{cd}(t_e^{10})] C_{8g}^{eff}(t_e^{10}) \right\}. \tag{62}
\end{aligned}$$

It is easy to see that the decay modes  $B_s^0 \rightarrow \pi^0 \eta_n, \pi^0 \eta_s, \eta_n \eta_n$  and  $\eta_n \eta_s$ , do not receive the NLO contributions from the quark-loop and the magnetic-penguin diagrams.

For other  $B_s \rightarrow PP$  decays involving no  $\eta^{(\prime)}$  mesons, the corresponding quark-loop and



magnetic penguin amplitudes are of the form

$$\begin{aligned}
\mathcal{M}_{\pi^- K^+}^{(q)} = & -8m_{B_s}^4 \frac{C_F^2}{\sqrt{2N_c}} \int_0^1 dx_1 dx_2 dx_3 \int_0^\infty b_1 db_1 b_3 db_3 \phi_{B_s}(x_1) \{ [(1+x_3)\phi_\pi^A(x_2)\phi_K^A(x_3) \\
& + 2r_\pi \phi_\pi^P(x_2)\phi_K^A(x_3) + r_K(1-2x_3)\phi_\pi(x_2)(\phi_K^P(x_3) + \phi_K^T(x_3)) \\
& + 2r_\pi r_K \phi_\pi^P(x_2)((2+x_3)\phi_K^P(x_3) - x_3\phi_K^T(x_3))] \\
& \cdot \alpha_s^2(t_e^9) h_e(x_1, x_3, b_1, b_3) \exp[-S_{ab}(t_e^9)] C^{(q)}(t_e^9, l^2) \\
& + [2r_K \phi_\pi^A(x_2)\phi_K^P(x_3) + 4r_\pi r_K \phi_\pi^P(x_2)\phi_K^P(x_3)] \\
& \cdot \alpha_s^2(t_e^{10}) h_e(x_3, x_1, b_3, b_1) \exp[-S_{ab}(t_e^{10})] C^{(q)}(t_e^{10}, l^2) \}, \tag{63}
\end{aligned}$$

$$\begin{aligned}
\mathcal{M}_{\pi^- K^+}^{(g)} = & -16m_{B_s}^6 \frac{C_F^2}{\sqrt{2N_c}} \int_0^1 dx_1 dx_2 dx_3 \int_0^\infty b_1 db_1 b_2 db_2 b_3 db_3 \phi_{B_s}(x_1) \\
& \cdot \{ [(1-x_3) [2\phi_K^A(x_3) + r_K(3\phi_K^P(x_3) + \phi_K^T(x_3)) \\
& + r_K x_3(\phi_K^P(x_3) - \phi_K^T(x_3))] \phi_\pi^A(x_2) \\
& - r_\pi x_2(1+x_3)(3\phi_\pi^P(x_2) - \phi_\pi^T(x_2))\phi_K^A(x_3) \\
& - r_\pi r_K(1-x_3)(3\phi_\pi^P(x_2) + \phi_\pi^T(x_2))(\phi_K^P(x_3) - \phi_K^T(x_3)) \\
& - r_\pi r_K x_2(1-2x_3)(3\phi_\pi^P(x_2) - \phi_\pi^T(x_2))(\phi_K^P(x_3) + \phi_K^T(x_3))] \\
& \cdot \alpha_s^2(t_e^9) h_g(x_1, x_2, x_3, b_1, b_2, b_3) \exp[-S_{cd}(t_e^9)] C_{8g}^{eff}(t_e^9) \\
& + [4r_K \phi_\pi^A(x_2)\phi_K^P(x_3) + 2r_\pi r_K x_2(3\phi_\pi^P(x_2) - \phi_\pi^T(x_2))\phi_K^P(x_3)] \\
& \alpha_s^2(t_e^{10}) h'_g(x_1, x_2, x_3, b_1, b_2, b_3) \exp[-S_{cd}(t_e^{10})] C_{8g}^{eff}(t_e^{10}) \}, \tag{64}
\end{aligned}$$

$$\mathcal{M}_{K^0 \pi^0}^{(q)} = \frac{1}{\sqrt{2}} \mathcal{M}_{\pi^- K^+}^{(q)}, \tag{65}$$

$$\mathcal{M}_{K^0 \pi^0}^{(g)} = \frac{1}{\sqrt{2}} \mathcal{M}_{\pi^- K^+}^{(g)}, \tag{66}$$

$$\begin{aligned}
\mathcal{M}_{K^+ K^-}^{(q)} = & -8m_{B_s}^4 \frac{C_F^2}{\sqrt{2N_c}} \int_0^1 dx_1 dx_2 dx_3 \int_0^\infty b_1 db_1 b_3 db_3 \phi_{B_s}(x_1) \\
& \cdot \{ [(1+x_3)\phi_k^A(x_2)\phi_K^A(x_3) + 2r_k \phi_k^P(x_2)\phi_K^A(x_3) \\
& + r_K(1-2x_3)\phi_k(x_2)(\phi_K^P(x_3) + \phi_K^T(x_3)) \\
& + 2r_k r_K \phi_k^P(x_2)((2+x_3)\phi_K^P(x_3) - x_3\phi_K^T(x_3))] \\
& \cdot \alpha_s^2(t_e^9) h_e(x_1, x_3, b_1, b_3) \exp[-S_{ab}(t_e^9)] C^{(q)}(t_e^9, l^2) \\
& + [2r_K \phi_k^A(x_2)\phi_K^P(x_3) + 4r_k r_K \phi_k^P(x_2)\phi_K^P(x_3)] \\
& \cdot \alpha_s^2(t_e^{10}) h_e(x_3, x_1, b_3, b_1) \exp[-S_{ab}(t_e^{10})] C^{(q)}(t_e^{10}, l^2) \}, \tag{67}
\end{aligned}$$

$$\begin{aligned}
\mathcal{M}_{K^+K^-}^{(g)} = & -16m_{B_s}^6 \frac{C_F^2}{\sqrt{2N_c}} \int_0^1 dx_1 dx_2 dx_3 \int_0^\infty b_1 db_1 b_2 db_2 b_3 db_3 \phi_{B_s}(x_1) \\
& \cdot \left\{ [(1-x_3) [2\phi_K^A(x_3) + r_K(3\phi_K^P(x_3) + \phi_K^T(x_3))] \right. \\
& + r_K x_3 (\phi_K^P(x_3) - \phi_K^T(x_3))] \phi_K^A(x_2) \\
& - r_K x_2 (1+x_3) (3\phi_K^P(x_2) - \phi_K^T(x_2)) \phi_K^A(x_3) \\
& - r_K^2 (1-x_3) (3\phi_K^P(x_2) + \phi_K^T(x_2)) (\phi_K^P(x_3) - \phi_K^T(x_3)) \\
& \left. - r_K^2 x_2 (1-2x_3) (3\phi_K^P(x_2) - \phi_K^T(x_2)) (\phi_K^P(x_3) + \phi_K^T(x_3))] \right. \\
& \cdot \alpha_s^2(t_e^9) h_g(x_1, x_2, x_3, b_1, b_2, b_3) \exp[-S_{cd}(t_e^9)] C_{8g}^{eff}(t_e^9) \\
& + [4r_K \phi_K^A(x_2) \phi_K^P(x_3) + 2r_K r_K x_2 (3\phi_K^P(x_2) - \phi_K^T(x_2)) \phi_K^P(x_3)] \\
& \left. \cdot \alpha_s^2(t_e^{10}) h'_g(x_1, x_2, x_3, b_1, b_2, b_3) \exp[-S_{cd}(t_e^{10})] C_{8g}^{eff}(t_e^{10}) \right\}, \tag{68}
\end{aligned}$$

$$\mathcal{M}_{\bar{K}^0 K^0}^{(q)} = \mathcal{M}_{k^+ k^-}^{(q)}, \tag{69}$$

$$\mathcal{M}_{\bar{K}^0 K^0}^{(g)} = \mathcal{M}_{k^+ k^-}^{(g)}. \tag{70}$$

The functions  $h_e, h_g, h'_g$ , the hard scales  $t_e^9$  and  $t_e^{10}$ , the Sudakov factors  $S_{ab}(t)$  and  $S_{cd}(t)$ , appeared in Eqs.(57)-(68), will be given in Appendix A.

For the pure annihilation-type decays  $B_s^0 \rightarrow \pi^+ \pi^-$  and  $B_s^0 \rightarrow \pi^0 \pi^0$ , they do not receive the NLO contributions from the vertex corrections, the quark loops and the magnetic penguins. For  $B_s^0 \rightarrow \pi^0 \eta$  and  $B_s^0 \rightarrow \pi^0 \eta'$  decays, the quark-loops and magnetic penguins also do not contribute. For other decays, the NLO contributions will be included in a simple way:

$$\begin{aligned}
\mathcal{A}_{\eta_n K^0} & \rightarrow \mathcal{A}_{\eta_n K^0} + \sum_{q=u,c,t} \xi_q \mathcal{M}_{\eta_n K^0}^{(q)} + \xi_t \mathcal{M}_{\eta_n K^0}^{(g)}, \\
\mathcal{A}_{K^0 \eta_s} & \rightarrow \mathcal{A}_{K^0 \eta_s} + \sum_{q=u,c,t} \xi_q \mathcal{M}_{K^0 \eta_s}^{(q)} + \xi_t \mathcal{M}_{K^0 \eta_s}^{(g)}, \\
\mathcal{A}_{\eta_s \eta_s} & \rightarrow \mathcal{A}_{\eta_s \eta_s} + \sum_{q=u,c,t} \xi'_q \mathcal{M}_{\eta_s \eta_s}^{(q)} + \xi'_t \mathcal{M}_{\eta_s \eta_s}^{(g)}, \\
\mathcal{A}_{\pi^- K^+} & \rightarrow \mathcal{A}_{\pi^- K^+} + \sum_{q=u,c,t} \xi_q \mathcal{M}_{\pi^- K^+}^{(q)} + \xi_t \mathcal{M}_{\pi^- K^+}^{(g)}, \\
\mathcal{A}_{\pi^0 K^0} & \rightarrow \mathcal{A}_{\pi^0 K^0} + \sum_{q=u,c,t} \xi_q \mathcal{M}_{\pi^0 K^0}^{(q)} + \xi_t \mathcal{M}_{\pi^0 K^0}^{(g)}, \\
\mathcal{A}_{K^- K^+} & \rightarrow \mathcal{A}_{K^- K^+} + \sum_{q=u,c,t} \xi'_q \mathcal{M}_{K^- K^+}^{(q)} + \xi'_t \mathcal{M}_{K^- K^+}^{(g)}, \\
\mathcal{A}_{\bar{K}^0 K^0} & \rightarrow \mathcal{A}_{\bar{K}^0 K^0} + \sum_{q=u,c,t} \xi'_q \mathcal{M}_{\bar{K}^0 K^0}^{(q)} + \xi'_t \mathcal{M}_{\bar{K}^0 K^0}^{(g)}, \tag{71}
\end{aligned}$$

where  $\xi_q = V_{qb} V_{qd}^*$ , and  $\xi'_q = V_{qb} V_{qs}^*$  with  $q = u, c, t$ .

## V. NUMERICAL RESULTS

In the numerical calculations the following input parameters will be used.

$$\begin{aligned}
\Lambda_{\overline{\text{MS}}}^{(5)} &= 0.225\text{GeV}, & f_{B_s} &= (0.23 \pm 0.02)\text{GeV}, & f_K &= 0.16\text{GeV}, \\
f_\pi &= 0.13\text{GeV}, & M_{B_s} &= 5.37\text{GeV}, & m_K &= 0.494\text{GeV}, & m_\eta &= 547.9\text{MeV}, \\
m'_\eta &= 0.958\text{GeV}, & m_0^\pi &= 1.4\text{GeV}, & m_0^K &= 1.9\text{GeV}, & \tau_{B_s^0} &= 1.470 \text{ ps}, \\
m_b &= 4.8\text{GeV}, & M_W &= 80.42\text{GeV}.
\end{aligned} \tag{72}$$

For the CKM matrix elements, we also take the same values as being used in Ref. [10], and neglect the small errors on  $V_{ud}, V_{us}, V_{ts}$  and  $V_{tb}$

$$\begin{aligned}
|V_{ud}| &= 0.974, & |V_{us}| &= 0.226, & |V_{ub}| &= (3.68_{-0.08}^{+0.11}) \times 10^{-3}, \\
|V_{td}| &= (8.20_{-0.27}^{+0.59}) \times 10^{-3}, & |V_{ts}| &= 40.96 \times 10^{-3}, & |V_{tb}| &= 1.0, \\
\alpha &= (99_{-9.4}^{+4})^\circ, & \gamma &= (59.0_{-3.7}^{+9.7})^\circ, & \arg[-V_{ts}V_{tb}^*] &= 1^\circ.
\end{aligned} \tag{73}$$

### A. Branching Ratios

For the considered  $\bar{B}_s^0 \rightarrow PP$  decays, the decay amplitude for a given decay mode with  $b \rightarrow d$  transition can be generally written as

$$\mathcal{A}(\bar{B}_s^0 \rightarrow f) = V_{ub}V_{ud}^*T - V_{tb}V_{td}^*P = V_{ub}V_{ud}^*T [1 + ze^{i(-\alpha+\delta)}], \tag{74}$$

where  $\alpha$  is the weak phase (one of the three CKM angles),  $\delta = \arg[P/T]$  is the relative strong phase between the ‘‘T’’ and ‘‘P’’ part, and the parameter ‘‘z’’ is defined as

$$z = \left| \frac{V_{tb}V_{td}^*}{V_{ub}V_{ud}^*} \right| \left| \frac{P}{T} \right|. \tag{75}$$

The ratio  $z$  and the strong phase  $\delta$  can be calculated in the pQCD approach. The CP-averaged branching ratio, consequently, can be defined as

$$\text{Br}(B_s^0 \rightarrow f) = \frac{G_F^2 \tau_{B_s^0}}{32\pi m_B} \frac{|\mathcal{A}(\bar{B}_s^0 \rightarrow f)|^2 + |\mathcal{A}(B_s^0 \rightarrow \bar{f})|^2}{2} \tag{76}$$

where  $\tau_{B_s^0}$  is the lifetime of the  $B_s$  meson.

For the case of  $b \rightarrow s$  transition, we have similarly

$$\mathcal{A}(\bar{B}_s^0 \rightarrow f) = V_{ub}V_{us}^*T' [1 + z'e^{i(\gamma+\delta)}], \tag{77}$$

where  $\gamma$  is also one of the three CKM angles,  $\delta = \arg[P'/T']$  is the relative strong phase, while the parameter ‘‘z’’ is defined as with

$$z' = \left| \frac{V_{tb}V_{ts}^*}{V_{ub}V_{us}^*} \right| \left| \frac{P'}{T'} \right| \tag{78}$$

In Table I we show the pQCD predictions for the CP-averaged branching ratios of the thirteen  $B_s \rightarrow PP$  decays. The label LO means the leading order pQCD predictions. The

TABLE I: Branching ratios ( $\times 10^{-6}$ ) of  $B_s \rightarrow PP$  decays in the pQCD approach. The label  $LO$  means the leading order pQCD predictions, while  $+VC, +QL, +MP$ , as well as  $NLO$  means that the vertex corrections, the quark loops, the magnetic penguins, and all the above  $NLO$  corrections are added to the  $LO$  results, respectively. The errors in the table are defined in the context. For comparison, we also cite the leading-order pQCD predictions as given in Ref. [10], the QCDF results in Ref. [6], and currently available data [21, 22, 23].

Mode	Class	LO	+ VC	+ QL	+ MP	NLO	pQCD[10]	QCDF[6]	Data
$\bar{B}_s^0 \rightarrow K^0 \eta$	$C$	0.10	0.08	0.12	0.10	$0.19^{+0.03+0.02+0.02}_{-0.06-0.00-0.04}$	$0.11^{+0.08}_{-0.11}$	$0.34^{+0.72}_{-0.33}$	
$\bar{B}_s^0 \rightarrow K^0 \eta'$	$C$	0.70	1.09	1.13	1.29	$1.87^{+0.34+0.27+0.13}_{-0.51-0.11-0.21}$	$0.72^{+0.36}_{-0.24}$	$2.0^{+2.2}_{-1.3}$	
$\bar{B}_s^0 \rightarrow \pi^0 \eta$	$P_{EW}$	0.04	0.03	—	—	$0.03^{+0.01+0.00+0.00}_{-0.00-0.00-0.01}$	$0.05^{+0.02}_{-0.02}$	$0.08^{+0.04}_{-0.03}$	
$\bar{B}_s^0 \rightarrow \pi^0 \eta'$	$P_{EW}$	0.09	0.08	—	—	$0.08^{+0.03+0.00+0.01}_{-0.02-0.00-0.01}$	$0.11^{+0.05}_{-0.03}$	$0.11^{+0.05}_{-0.05}$	
$\bar{B}_s^0 \rightarrow \eta \eta$	$P$	7.4	7.8	9.1	12.0	$10.0^{+3.3+0.0+0.6}_{-2.5-0.03-0.8}$	$8.0^{+5.4}_{-3.1}$	$15.6^{+17.0}_{-9.2}$	
$\bar{B}_s^0 \rightarrow \eta \eta'$	$P$	21.6	31.7	28.6	37.4	$34.9^{+11.3+0.03+2.8}_{-8.6-0.1-4.1}$	$21.0^{+11.7}_{-7.2}$	$54.0^{+52.8}_{-29.1}$	
$\bar{B}_s^0 \rightarrow \eta' \eta'$	$P$	14.9	30.3	18.9	27.1	$25.2^{+8.1+0.1+1.9}_{-6.1-0.0-2.3}$	$14.0^{+7.0}_{-4.1}$	$41.7^{+47.5}_{-24.9}$	
$\bar{B}_s^0 \rightarrow K^+ \pi^-$	$T$	7.0	6.3	6.1	6.0	$6.3^{+2.5+0.5+0.4}_{-1.8-0.5-0.3}$	$7.6^{+3.3}_{-2.5}$	$10.2^{+6.0}_{-5.2}$	$5.0 \pm 1.3$
$\bar{B}_s^0 \rightarrow K^0 \pi^0$	$C$	0.16	0.30	0.18	0.18	$0.25^{+0.09+0.03+0.02}_{-0.06-0.01-0.03}$	$0.16^{+0.12}_{-0.07}$	$0.49^{+0.62}_{-0.35}$	
$\bar{B}_s^0 \rightarrow \pi^+ \pi^-$	$ann$	0.70	—	—	—	$0.57^{+0.14+0.01+0.20}_{-0.11-0.00-0.19}$	$0.57^{+0.18}_{-0.16}$	$0.02^{+0.17}_{-0.02}$	$0.53 \pm 0.51$
$\bar{B}_s^0 \rightarrow \pi^0 \pi^0$	$ann$	0.35	—	—	—	$0.29^{+0.07+0.01+0.10}_{-0.06-0.00-0.10}$	$0.28^{+0.09}_{-0.08}$	$0.01^{+0.08}_{-0.01}$	
$\bar{B}_s^0 \rightarrow K^+ K^-$	$P$	11.8	15.5	16.0	15.4	$15.6^{+5.0+0.7+0.8}_{-3.8-0.3-0.7}$	$13.6^{+8.6}_{-5.2}$	$22.7^{+27.8}_{-13.0}$	$24.4 \pm 4.8$
$\bar{B}_s^0 \rightarrow \bar{K}^0 K^0$	$P$	14.3	17.2	18.0	17.5	$18.0^{+4.6+0.0+0.7}_{-5.9-0.0-0.6}$	$15.6^{+9.7}_{-6.0}$	$24.7^{+29.4}_{-14.0}$	

label  $+VC, +QL, +MP$ , and  $NLO$  means that the vertex corrections, the quark loops, the magnetic penguins, and all the considered  $NLO$  corrections are included, respectively. The errors as shown for the  $NLO$  pQCD predictions correspond to the uncertainties of the various input parameters. The first error comes from  $\omega_b = 0.50 \pm 0.05$  and  $f_{B_s} = 0.23 \pm 0.02$  GeV. The second error arises from the uncertainties of the CKM matrix elements  $|V_{ub}|$  and  $|V_{cb}|$ , as well as the CKM angles  $\alpha$  and  $\gamma$  as given in Eq. (73). The first two errors are defined in a similar way as that in Ref. [10]. The third error comes from the uncertainties of relevant Gegenbauer moments:  $a_1^K = 0.17 \pm 0.05$ ,  $a_2^K = 0.20 \pm 0.06$  and  $a_2^\pi = 0.44^{+0.10}_{-0.20}$ . We here assign roughly a 30% uncertainty for Gegenbauer moments to estimate the resultant effects on the theoretical predictions of the branching ratios.

For the sake of comparison, we also list the leading order pQCD predictions as given in Ref. [10] and the theoretical predictions based on the QCD factorization approach [6] in Table I. The corresponding errors of the previous LO pQCD and QCDF predictions denote the combined error: the individual errors as given in Refs. [6, 10] are added in quadrature. The currently available experimental measurements [21, 22, 23] are also shown in the last column of Table I.

From the numerical results about the branching ratios, one can see that

- The LO pQCD predictions for branching ratios of  $\bar{B}_s \rightarrow PP$  decays as given in Ref. [10] are confirmed by our independent calculation. The very small differences are induced by the different choices of the scales  $\Lambda_{QCD}^{(4)}$  and  $\Lambda_{QCD}^{(5)}$ : we take  $\Lambda_{QCD}^{(5)} = 0.225$  GeV and the corresponding  $\Lambda_{QCD}^{(4)} = 0.287$  GeV, instead of the values of

$\Lambda_{QCD}^{(5)} = 0.193$  GeV and  $\Lambda_{QCD}^{(4)} = 0.25$  GeV as being used in Ref. [10].

- In this paper, the NLO contributions are taken into account partially. The considered NLO contributions can interfere with the LO part constructively or destructively for different decay modes. For most decays the changes of the LO results are moderate and reasonable. The theoretical uncertainty from  $\omega_b = 0.50 \pm 0.05$  is dominant, while the error from the uncertainty of CKM elements is small. And the total theoretical error is in general around 30% to 50% in size.
- For the “tree” dominated decay  $\bar{B}_s \rightarrow K^+\pi^-$ , the NLO pQCD prediction agrees with the data within one standard deviation. The agreement between the pQCD prediction and the measured value is improved due to the inclusion of the considered NLO contribution.
- For the three “Color-suppressed” decays, the NLO enhancement can be significant, from  $\sim 50\%$  for the  $\bar{B}_s \rightarrow K^0\eta$  and  $K^0\pi^0$  decays to  $\sim 170\%$  for the  $\bar{B}_s \rightarrow K^0\eta'$  decay. The differences between the LO pQCD predictions and the QCDF predictions become narrow obviously because of the inclusion of the NLO contributions.
- For the five “QCD-Penguin” decays  $\bar{B}_s \rightarrow \eta^{(\prime)}\eta^{(\prime)}$  and  $KK$  decays, the enhancements due to the considered NLO contributions can be as large as (30 – 70)%, which are helpful to pin down the gap between the pQCD and the QCDF predictions.
- For the two “Electroweak-Penguin” decays  $\bar{B}_s \rightarrow \pi^0\eta^{(\prime)}$ , the NLO contributions are small. The pQCD predictions agree well with the QCDF predictions.
- For the “annihilation” decays  $\bar{B}_s \rightarrow \pi^+\pi^-$  and  $\pi^0\pi^0$  decays, the NLO contributions are around 10% only. The pQCD predictions agree well with the measured value.
- For the considered thirteen  $B_s \rightarrow PP$  decays, only three of them,  $B_s \rightarrow K^+\pi^-, K^+K^-$  and  $\pi^+\pi^-$ , have been measured experimentally with good precision. It is easy to see that the consistency between the pQCD predictions for their branching ratios and the measured values will be improved effectively when the NLO contributions are included.

## B. CP-violating asymmetries

Now we turn to the evaluations of the CP-violating asymmetries of  $B_s \rightarrow PP$  decays in pQCD approach. Restricting the final state  $f$  to have definite CP, the time-dependent decay width for the  $B_s \rightarrow f$  decay can be written as [24]

$$\Gamma(\bar{B}_s^0(t) \rightarrow f) = e^{-\Gamma t} \bar{\Gamma}(\bar{B}_s^0 \rightarrow f) \cdot \left[ \cosh\left(\frac{\Delta\Gamma t}{2}\right) + H_f \sinh\left(\frac{\Delta\Gamma t}{2}\right) + \mathcal{A}_{CP}^{dir} \cos(\Delta m t) + S_f \sin(\Delta m t) \right] \quad (79)$$

where  $\Delta m = m_H - m_L > 0$ ,  $\bar{\Gamma} = (\Gamma_H + \Gamma_L)/2$  is the average decay widths, while  $\Delta\Gamma = \Gamma_H - \Gamma_L$  is the difference of decay widths for the heavier and lighter  $B_s^0$  mass eigenstates.

TABLE II: Direct CP asymmetries(in %) of  $B_s \rightarrow PP$  decays in the pQCD approach. The label  $LO$  means the leading order pQCD predictions, while  $+VC$ ,  $+QL$ ,  $+MP$ , as well as  $NLO$  means that the vertex corrections, the quark loops, the magnetic penguins, and all the above  $NLO$  corrections are added to the  $LO$  results, respectively. The errors in the table are defined in the context. For comparison, we also cite the leading-order pQCD predictions as given in Ref. [10], the QCDF results in Ref. [6].

Mode	Class	LO	+ VC	+ QL	+ MP	NLO	pQCD[10]	QCDF[6]
$\bar{B}_s^0 \rightarrow K^0 \eta$	$C$	65.0	45.4	38.6	30.7	$96.7^{+0.0+1.1+1.2}_{-0.1-2.0-1.5}$	$56.4^{+8.0}_{-9.3}$	$46.8^{+48.8}_{-58.8}$
$\bar{B}_s^0 \rightarrow K^0 \eta'$	$C$	-22.3	-5.7	-18.1	-0.8	$-35.4^{+2.0+2.4+0.5}_{-0.0-2.5-0.3}$	$-19.9^{+5.5}_{-5.3}$	$-36.6^{+22.3}_{-20.7}$
$\bar{B}_s^0 \rightarrow \pi^0 \eta$	$P_{EW}$	0.3	40.4	-	-	$40.4^{+0.3+1.6+3.6}_{-0.8-1.3-7.2}$	$-0.4^{+0.3}_{-0.3}$	-
$\bar{B}_s^0 \rightarrow \pi^0 \eta'$	$P_{EW}$	23.8	52.5	-	-	$52.5^{+2.0+2.4+0.5}_{-0.0-2.5-0.3}$	$20.6^{+3.4}_{-2.9}$	$27.8^{+27.2}_{-28.8}$
$\bar{B}_s^0 \rightarrow \eta \eta$	$P$	-0.7	-1.53	1.2	1.1	$0.6^{+0.1+0.1+0.2}_{-0.0-0.0-0.0}$	$-0.6^{+0.6}_{-0.5}$	$-1.6^{+2.4}_{-2.4}$
$\bar{B}_s^0 \rightarrow \eta \eta'$	$P$	-1.3	-1.1	-0.2	-0.6	$-0.2^{+0.1+0.0+0.1}_{-0.1-0.0-0.1}$	$-1.3^{+0.1}_{-0.2}$	$0.4^{+0.5}_{-0.4}$
$\bar{B}_s^0 \rightarrow \eta' \eta'$	$P$	1.9	1.3	1.0	1.3	$1.4^{+0.1+0.1+0.1}_{-0.1-0.1-0.2}$	$1.9^{+0.4}_{-0.5}$	$2.1^{+1.3}_{-1.4}$
$\bar{B}_s^0 \rightarrow K^+ \pi^-$	$T$	25.7	28.6	25.7	28.5	$25.8^{+4.1+1.5+2.7}_{-3.8-0.7-5.0}$	$24.1^{+5.6}_{-4.8}$	$-6.7^{+15.6}_{-15.3}$
$\bar{B}_s^0 \rightarrow K^0 \pi^0$	$C$	66.9	86.4	-18.7	-10.8	$88.0^{+3.7+2.6+1.6}_{-4.5-6.7-1.6}$	$59.4^{+7.9}_{-12.5}$	$42^{+47}_{-56}$
$\bar{B}_s^0 \rightarrow \pi^+ \pi^-$	$ann$	-1.1	-	-	-	$0.2^{+0.1+0.0+2.0}_{-0.0-0.0-1.5}$	$-1.2^{+1.2}_{-1.3}$	-
$\bar{B}_s^0 \rightarrow \pi^0 \pi^0$	$ann$	-1.1	-	-	-	$0.2^{+0.1}_{-1.5}$	$-1.2^{+1.2}_{-1.2}$	-
$\bar{B}_s^0 \rightarrow K^+ K^-$	$P$	-22.1	-17.9	-14.1	-17.1	$-15.6^{+1.2+0.7+1.3}_{-0.8-0.9-1.1}$	$-23.3^{+5.0}_{-4.6}$	$4.0^{+10.6}_{-11.6}$
$\bar{B}_s^0 \rightarrow \bar{K}^0 K^0$	$P$	0	0	0.3	0	$0.4 \pm 0.1$	0	$0.9 \pm 0.4$

In the  $B_s$  system, we expect a much larger decay width difference:  $(\Delta\Gamma/\Gamma)_{B_s} \sim -20\%$  [21]. Besides  $\mathcal{A}^{dir}$ , the CP-violating asymmetry  $S_f$  and  $H_f$  can be defined as

$$\mathcal{A}_{CP}^{dir} = \frac{|\lambda|^2 - 1}{1 + |\lambda|^2}, \quad S_f = \frac{2\text{Im}[\lambda]}{1 + |\lambda|^2}, \quad H_f = \frac{2\text{Re}[\lambda]}{1 + |\lambda|^2}, \quad (80)$$

with the parameter  $\lambda$

$$\lambda = \eta_f e^{2i\epsilon} \frac{A(\bar{B}_s \rightarrow f)}{A(B_s \rightarrow f)}, \quad (81)$$

where  $\eta_f$  is  $+1(-1)$  for a CP-even(CP-odd) final state  $f$  and  $\epsilon = \arg[-V_{ts}V_{tb}^*]$  is very small in size.

If we neglect the very small parameter  $\epsilon$ , the CP-violating asymmetries can be written explicitly as

$$\begin{aligned} \mathcal{A}_{CP}^{dir} &= \frac{2z \sin \alpha \sin \delta}{1 + 2z \cos \alpha \cos \delta + z^2}, \\ S_f &= -\frac{\sin(2\gamma) + z^2 \sin(2\gamma + 2\alpha) + 2z \cos \delta \sin(\alpha + 2\gamma)}{1 + z^2 + 2z \cos \delta \cos \alpha}, \\ H_f &= \frac{2z \cos(\delta) \cos(\alpha + 2\gamma) + \cos(2\gamma) + z^2 \cos(2\alpha + 2\gamma)}{1 + z^2 + 2z \cos \delta \cos \alpha}, \end{aligned} \quad (82)$$

for the decays relevant to the  $b \rightarrow d$  transition, and

$$\begin{aligned}
\mathcal{A}_{CP}^{dir} &= -\frac{2z' \sin \gamma \sin \delta}{1 + 2z' \cos \gamma \cos \delta + z'^2}, \\
S_f &= -\frac{\sin(2\gamma) + 2z' \cos \delta \sin \gamma}{1 + z'^2 + 2z' \cos \delta \cos \gamma}, \\
H_f &= \frac{z'^2 + 2z' \cos \delta \cos \gamma + \cos(2\gamma)}{1 + z'^2 + 2z' \cos \delta \cos \gamma},
\end{aligned} \tag{83}$$

for the case of  $b \rightarrow s$  transition.

The pQCD predictions for the direct CP asymmetries  $\mathcal{A}^{dir}$ , the mixing-induced CP asymmetries  $S_f$  and  $H_f$  of the considered  $B_s^0 \rightarrow PP$  decays are listed in Table II and Table III. In both tables, the label LO means the leading order pQCD predictions, and the labels +VC, +QL, +MP, as well as NLO mean that the vertex corrections, the quark loops, the magnetic penguins, and all the above NLO corrections are added to LO results, respectively. As a comparison, the LO pQCD predictions as given in Ref. [10] are listed in Table II and Table III. In Table II, the QCDF predictions for direct CP-violating asymmetries as given in Ref. [6] are also shown. The corresponding errors of the previous LO pQCD predictions and QCDF predictions are the combined errors: the individual errors as given in Refs. [6, 10] are added in quadrature. The errors of our NLO pQCD predictions for CP-violating asymmetries are defined in the same way as those for the branching ratios.

For the experimental measurements, there is only one measured CP asymmetry as reported by CDF Collaboration [22]:

$$\mathcal{A}_{CP}^{dir}(\bar{B}_s \rightarrow K^+ \pi^-) = 0.39 \pm 0.17. \tag{84}$$

But more data will become available soon when the LHC starts its physics running.

From the pQCD predictions and currently available experimental measurements for the CP violating asymmetries of the thirteen  $B \rightarrow PP$  decays, one can see the following points:

- The LO pQCD predictions obtained in this paper agree very well with those as given in Ref. [10]. For  $\bar{B}_s \rightarrow K^0 \eta$  and  $\pi^0 \eta$  decays, the LO pQCD predictions can be changed significantly by the inclusion of the NLO contributions. For other decays, the NLO contributions are small or moderate in size. The pQCD predictions are in general consistent with those in QCDF approach, but much larger than the later one for  $\bar{B}_s \rightarrow K^\eta, \pi^0 \eta'$  and  $K^0 \pi^0$  decays.
- For the “Tree” dominated decay  $\bar{B}_s \rightarrow K^+ \pi^-$ , the pQCD prediction for the direct CP asymmetry is  $\mathcal{A}_{CP}^{dir}(\bar{B}_s \rightarrow K^+ \pi^-) = 0.30 \pm 0.06$ , which agrees very well with the experimental measurement as given in Eq. (84). The QCDF prediction, however, is about  $-0.07 \pm 0.16$  and much different from the measured value.
- For the four “QCD-penguin” decays  $\bar{B}_s \rightarrow \eta^{(\prime)} \eta^{(\prime)}$  and  $\bar{K}^0 K^0$  decays, analogous to the QCDF predictions, the LO and NLO pQCD predictions for both  $\mathcal{A}_{CP}^{dir}$  and  $S_f$  are all very small in size.

TABLE III: The mixing-induced CP asymmetries (in %)  $S_f$  and  $H_f$  (the second row). The label LO means the leading order pQCD predictions, and the labels +VC, +QL, +MP, as well as NLO mean that the vertex corrections, the quark loops, the magnetic penguins, and all the above NLO corrections are added to LO results, respectively. The errors of the entries are defined in the context. As a comparison, the LO pQCD predictions as given in Ref. [10] are also listed.

Mode	Class	LO	+VC	+QL	+MP	NLO	pQCD[10]
$\bar{B}_s^0 \rightarrow K_s^0 \eta$	$C$	-37	-89	-92	-90	$-18_{-2-11-5}^{+0+7+3}$	$-43_{-23}^{+23}$
		-67	-57	6	32	$-18_{-0-8-9}^{+2+18+15}$	$-70_{-22}^{+14}$
$\bar{B}_s^0 \rightarrow K_s^0 \eta'$	$C$	-67	-59	-44	-53	$-46_{-0-23-0}^{+1+12+1}$	$-68_{-5}^{+6}$
		-70	-80	-88	-85	$-82_{-1-6-0}^{+0+20+1}$	$-70_{-7}^{+6}$
$\bar{B}_s^0 \rightarrow \pi^0 \eta$	$P_{EW}$	18	28	-	-	$28_{-3-1-4}^{+2+3+4}$	$17_{-13}^{+18}$
		98	87	-	-	$87_{-1-1-2}^{+1+1+4}$	$99_{-2}^{+1}$
$\bar{B}_s^0 \rightarrow \pi^0 \eta'$	$P_{EW}$	-25	-18	-	-	$-18_{-0-23-0}^{+1+12+1}$	$-17_{-9}^{+8}$
		94	83	-	-	$83_{-1-1-0}^{+3+17+1}$	$96_{-2}^{+2}$
$\bar{B}_s^0 \rightarrow \eta \eta$	$P$	3	0	1	1	$2_{-0-0-0}^{+0+0+0}$	$3_{-1}^{+1}$
		100	100	100	100	$100_{-0-0-0}^{+0+0+0}$	$100_{-0}^{+0}$
$\bar{B}_s^0 \rightarrow \eta \eta'$	$P$	4	3	4	3	$4_{-0-0-0}^{+0+0+0}$	$4_{-0}^{+0}$
		100	100	100	100	$100_{-0-0-0}^{+0+0+0}$	$100_{-0}^{+0}$
$\bar{B}_s^0 \rightarrow \eta' \eta'$	$P$	4	6	6	6	$5_{-1-1-0}^{+0+0+0}$	$4_{-1}^{+1}$
		100	100	100	100	$100_{-0-0-0}^{+0+0+0}$	$100_{-0}^{+0}$
$\bar{B}_s^0 \rightarrow K_s^0 \pi^0$	$C$	-55	-25	-98	-97	$-41_{-9-8-5}^{+8+4+3}$	$-61_{-20}^{+24}$
		-50	-44	-8	-20	$-23_{-1-18-7}^{+0+19+3}$	$-52_{-17}^{+23}$
$\bar{B}_s^0 \rightarrow K^+ K^-$	$P$	24	20	22	20	$22_{-2-1-2}^{+2+2+2}$	$28_{-5}^{+5}$
		95	96	96	96	$96_{-3-1-0}^{+4+0+0}$	$93_{-3}^{+3}$
$\bar{B}_s^0 \rightarrow \bar{K}^0 K^0$	$P$	-	-	0.4	-	$0.4_{-0-0-0}^{+0+0+0}$	4
		-	-	100	-	$100_{-0-0-0}^{+0+0+0}$	100
$\bar{B}_s^0 \rightarrow \pi^+ \pi^-$	$ann$	9.5	-	-	-	$9_{-0-0-0}^{+1+1+1}$	$14_{-6}^{+12}$
		99.5	-	-	-	$100_{-0-0-0}^{+0+0+0}$	$99_{-1}^{+0}$
$\bar{B}_s^0 \rightarrow \pi^0 \pi^0$	$ann$	9.5	-	-	-	$8.1_{-0.3-0.7-0.0}^{+0.1+0.5+0.3}$	$14_{-6}^{+12}$
		99.5	-	-	-	$100_{-0-0-0}^{+0+0+0}$	$99_{-1}^{+0}$

- For the “annihilation” decays  $\bar{B}_s \rightarrow \pi^+ \pi^-$  and  $\pi^0 \pi^0$ , the pQCD predictions for the direct CP-violating asymmetries are very small in size, while  $S_f$  is around 10% and  $H_f \sim 1$ .

## VI. SUMMARY

In this paper, we calculated the partial NLO contributions to the branching ratios and CP-violating asymmetries of  $\bar{B}_s^0 \rightarrow PP$  decays. Here the NLO contributions from the QCD vertex corrections, the quark-loops and the chromo-magnetic penguins are included.

From our calculations and phenomenological analysis, we found the following results:



- The LO pQCD predictions for the branching ratios and CP-violating asymmetries of  $B_s \rightarrow PP$  decays as presented in Ref. [10] are confirmed by our independent calculation.
- For branching ratios, the effects of the considered NLO contributions are varying from small to significant for different decay mode. For the three measured decays  $\bar{B}_s \rightarrow K^+\pi^-$ ,  $K^+K^-$  and  $\pi^+\pi^-$ , for example, the consistency between the pQCD predictions and the measured values are improved effectively due to the inclusion of the considered NLO contributions. For the three ‘‘Color-suppressed’’ decays, for instance, the NLO enhancement can be significant, from  $\sim 50\%$  for the  $\bar{B}_s \rightarrow K^0\eta$  and  $K^0\pi^0$  decays to  $\sim 170\%$  for the  $\bar{B}_s \rightarrow K^0\eta'$  decay, to be tested by forthcoming LHC experiments.
- As for the CP-violating asymmetries, the LO pQCD predictions for  $\bar{B}_s \rightarrow K^0\eta$  and  $\pi^0\eta$  decays could be changed significantly by the inclusion of the NLO contributions. For other decays, the NLO contributions are small or moderate in size. For  $\bar{B}_s \rightarrow K^+\pi^-$  decay, the pQCD prediction for the direct CP asymmetry is  $\mathcal{A}_{CP}^{dir}(\bar{B}_s \rightarrow K^+\pi^-) = 0.26 \pm 0.06$ , which agrees very well with the measured value  $\mathcal{A}_{CP}^{dir}(\bar{B}_s \rightarrow K^+\pi^-) = 0.39 \pm 0.17$ .
- In this paper, only the partial NLO contributions in the pQCD approach have been taken into account. The still missing pieces relevant with the emission diagrams, hard-spectator and annihilation diagrams should be evaluated as soon as possible.

## Acknowledgments

The authors would like to thank Cai-Dian Lü, Li-bo Guo, Zhi-qing Zhang, Xin Liu and Po Li for helpful discussions. This work is partly supported by the National Natural Science Foundation of China under Grant No.10575052, 10605012 and 10735080.

## APPENDIX A: RELATED FUNCTIONS

We show here the hard function  $h_i$  and the Sudakov factors  $S_{ab,cd,ef,gh}(t)$  appeared in the expressions of the decay amplitudes in Sec. III and IV. The hard functions  $h_i(x_j, b_j)$  are obtained by making the Fourier transformations of the hard kernel  $H^{(0)}$ .

$$h_e(x_1, x_3, b_1, b_3) = [\theta(b_1 - b_3)I_0(\sqrt{x_3}M_{B_s}b_3)K_0(\sqrt{x_3}M_{B_s}b_1) + \theta(b_3 - b_1)I_0(\sqrt{x_3}M_{B_s}b_1) \times K_0(\sqrt{x_3}M_{B_s}b_3)]K_0(\sqrt{x_1x_3}M_{B_s}b_1)S_t(x_3), \quad (\text{A1})$$

$$h_n(x_i, b_1, b_2) = [\theta(b_2 - b_1)K_0(M_{B_s}\sqrt{x_1x_3}b_2)I_0(M_{B_s}\sqrt{x_1x_3}b_1) + \theta(b_1 - b_2)K_0(M_{B_s}\sqrt{x_1x_3}b_1)I_0(M_{B_s}\sqrt{x_1x_3}b_2)] \times \begin{cases} \frac{i\pi}{2}H_0^{(1)}\left(M_{B_s}\sqrt{(x_2 - x_1)x_3}b_2\right), & \text{for } x_1 - x_2 < 0, \\ K_0\left(M_{B_s}\sqrt{(x_2 - x_1)x_3}b_2\right), & \text{for } x_2 - x_1 > 0, \end{cases} \quad (\text{A2})$$

$$h_a(x_2, x_3, b_2, b_3) = [\theta(b_2 - b_3)K_0(i\sqrt{x_3}M_{B_s}b_2)I_0(i\sqrt{x_3}M_{B_s}b_3) + \theta(b_3 - b_2) \\ \times K_0(i\sqrt{x_3}M_{B_s}b_3)I_0(i\sqrt{x_3}M_{B_s}b_2)]K_0(i\sqrt{x_2x_3}M_{B_s}b_2)S_t(x_3), \quad (\text{A3})$$

$$h_{na}(x_i, b_1, b_2) = \left[ \theta(b_1 - b_2)K_0\left(i\sqrt{x_2(1-x_3)}M_{B_s}b_1\right)I_0\left(i\sqrt{x_2(1-x_3)}M_{B_s}b_2\right) \right. \\ \left. + \theta(b_2 - b_1)K_0\left(i\sqrt{x_2(1-x_3)}M_{B_s}b_2\right)I_0\left(i\sqrt{x_2(1-x_3)}M_{B_s}b_1\right) \right] \\ \times K_0\left(\sqrt{1-(1-x_1-x_2)x_3}M_{B_s}b_2\right), \quad (\text{A4})$$

$$h'_{na}(x_i, b_1, b_2) = \left[ \theta(b_1 - b_2)K_0\left(i\sqrt{x_2(1-x_3)}M_{B_s}b_1\right)I_0\left(i\sqrt{x_2(1-x_3)}M_{B_s}b_2\right) \right. \\ \left. + \theta(b_2 - b_1)K_0\left(i\sqrt{x_2(1-x_3)}M_{B_s}b_2\right)I_0\left(i\sqrt{x_2(1-x_3)}M_{B_s}b_1\right) \right] \\ \times \begin{cases} \frac{i\pi}{2}H_0^{(1)}\left(M_{B_s}\sqrt{(x_2-x_1)(1-x_3)}b_1\right), & \text{for } x_1 - x_2 < 0, \\ K_0\left(M_{B_s}\sqrt{(x_2-x_1)(1-x_3)}b_1\right), & \text{for } x_2 - x_1 > 0, \end{cases} \quad (\text{A5})$$

$$h_g(x_i, b_i) = -\frac{i\pi}{2}S_t(x_3) \left[ J_0(\sqrt{x_2x_3}M_{B_s}b_2) + iN_0(\sqrt{x_2x_3}M_{B_s}b_2) \right] K_0(\sqrt{x_1x_3}M_{B_s}b_1) \\ \cdot \int_0^{\pi/2} d\theta \tan\theta \cdot J_0(\sqrt{x_3}M_{B_s}b_1 \tan\theta) J_0(\sqrt{x_3}M_{B_s}b_2 \tan\theta) \\ \cdot J_0(\sqrt{x_3}M_{B_s}b_3 \tan\theta), \quad (\text{A6})$$

$$h'_g(x_i, b_i) = -S_t(x_1)K_0(\sqrt{x_1x_3}M_{B_s}b_3) \cdot \int_0^{\pi/2} d\theta \tan\theta \cdot J_0(\sqrt{x_1}M_{B_s}b_1 \tan\theta) \\ \cdot J_0(\sqrt{x_1}M_{B_s}b_2 \tan\theta) J_0(\sqrt{x_1}M_{B_s}b_3 \tan\theta) \\ \times \begin{cases} \frac{i\pi}{2} \left[ J_0(\sqrt{x_2-x_1}M_{B_s}b_2) + iN_0(\sqrt{x_2-x_1}M_{B_s}b_2) \right], & x_1 < x_2, \\ K_0(\sqrt{x_1-x_2}M_{B_s}b_2), & x_1 > x_2, \end{cases} \quad (\text{A7})$$

where

$$K_0(ix) = \frac{i\pi}{2}H_0^{(1)}(x) = \frac{i\pi}{2} [iY_0(x) + J_0(x)], \quad (\text{A8})$$

with  $K_0$ ,  $I_0$  and  $J_0$  are the Bessel functions [25]. And the threshold resummation form factor  $S_t(x_i)$  can be found in Ref. [26].

The Sudakov factors appeared in Eqs. (37-46) are defined as

$$S_{ab}(t) = s\left(x_1\frac{m_{B_s}}{\sqrt{2}}, b_1\right) + s\left(x_3\frac{m_{B_s}}{\sqrt{2}}, b_3\right) + s\left(\bar{x}_3\frac{m_{B_s}}{\sqrt{2}}, b_3\right) \\ + \frac{5}{3} \int_{1/b_1}^t d\mu \frac{\gamma_q(\alpha_s(\mu))}{\mu} + 2 \int_{1/b_3}^t d\mu \frac{\gamma_q(\alpha_s(\mu))}{\mu}, \quad (\text{A9})$$

$$\begin{aligned}
S_{cd}(t) = & s\left(x_1 \frac{m_{B_s}}{\sqrt{2}}, b_1\right) + s\left(x_2 \frac{m_{B_s}}{\sqrt{2}}, b_2\right) + s\left(\bar{x}_2 \frac{m_{B_s}}{\sqrt{2}}, b_2\right) + s\left(x_3 \frac{m_{B_s}}{\sqrt{2}}, b_1\right) \\
& + s\left(\bar{x}_3 \frac{m_{B_s}}{\sqrt{2}}, b_1\right) + \frac{11}{3} \int_{1/b_1}^t d\mu \frac{\gamma_q(\alpha_s(\mu))}{\mu} + 2 \int_{1/b_2}^t d\mu \frac{\gamma_q(\alpha_s(\mu))}{\mu}, \quad (\text{A10})
\end{aligned}$$

$$\begin{aligned}
S_{ef}(t) = & s\left(x_2 \frac{m_{B_s}}{\sqrt{2}}, b_2\right) + s\left(\bar{x}_2 \frac{m_{B_s}}{\sqrt{2}}, b_2\right) + s\left(x_3 \frac{m_{B_s}}{\sqrt{2}}, b_3\right) \\
& + s\left(\bar{x}_3 \frac{m_{B_s}}{\sqrt{2}}, b_3\right) + 2 \int_{1/b_2}^t d\mu \frac{\gamma_q(\alpha_s(\mu))}{\mu} + 2 \int_{1/b_3}^t d\mu \frac{\gamma_q(\alpha_s(\mu))}{\mu}, \quad (\text{A11})
\end{aligned}$$

$$\begin{aligned}
S_{gh}(t) = & s\left(x_1 \frac{m_{B_s}}{\sqrt{2}}, b_1\right) + s\left(x_2 \frac{m_{B_s}}{\sqrt{2}}, b_2\right) + s\left(\bar{x}_2 \frac{m_{B_s}}{\sqrt{2}}, b_2\right) + s\left(x_3 \frac{m_{B_s}}{\sqrt{2}}, b_2\right) \\
& + s\left(\bar{x}_3 \frac{m_{B_s}}{\sqrt{2}}, b_2\right) + \frac{5}{3} \int_{1/b_1}^t d\mu \frac{\gamma_q(\alpha_s(\mu))}{\mu} + 4 \int_{1/b_2}^t d\mu \frac{\gamma_q(\alpha_s(\mu))}{\mu}, \quad (\text{A12})
\end{aligned}$$

where the quark anomalous dimension  $\gamma_q = -\alpha_s/\pi$  and the function  $s(Q, b)$  is given as [27, 28]:

$$s(Q, b) = \int_{1/b}^Q \frac{d\mu}{\mu} \left[ \ln\left(\frac{Q}{\mu}\right) A(\alpha_s(\mu)) + B(\alpha_s(\mu)) \right] \quad (\text{A13})$$

with

$$\begin{aligned}
A &= \frac{4}{3} \frac{\alpha_s}{\pi} + \left[ \frac{67}{9} - \frac{\pi^2}{3} - \frac{10}{27} N_f + \frac{2}{3} \beta_0 \ln\left(\frac{e^{\gamma_E}}{2}\right) \right] \left(\frac{\alpha_s}{\pi}\right)^2, \\
B &= \frac{2}{3} \frac{\alpha_s}{\pi} \ln\left(\frac{e^{2\gamma_E-1}}{2}\right), \quad (\text{A14})
\end{aligned}$$

where  $\gamma_E = 0.57722 \dots$  is the Euler constant, an  $N_f$  is the number of active quark flavors. The hard scales  $t_e^i$  appeared in the above equations take the form of

$$\begin{aligned}
t_e^1 &= \max\{\sqrt{x_3} M_{B_s}, 1/b_1, 1/b_3\}, \\
t_e^2 &= \max\{\sqrt{x_1} M_{B_s}, 1/b_1, 1/b_3\}, \\
t_e^3 &= \max\left\{\sqrt{x_1 x_3} M_{B_s}, \sqrt{|1 - x_1 - x_2| x_3} M_{B_s}, 1/b_1, 1/b_2\right\}, \\
t_e^4 &= \max\left\{\sqrt{x_1 x_3} M_{B_s}, \sqrt{|x_1 - x_2| x_3} M_{B_s}, 1/b_1, 1/b_2\right\}, \\
t_e^5 &= \max\{\sqrt{\bar{x}_3} M_{B_s}, 1/b_2, 1/b_3\}, \\
t_e^6 &= \max\{\sqrt{\bar{x}_2} M_{B_s}, 1/b_2, 1/b_3\}, \\
t_e^7 &= \max\left\{\sqrt{x_2 \bar{x}_3} M_{B_s}, \sqrt{1 - (1 - x_1 - x_2) x_3} M_{B_s}, 1/b_1, 1/b_2\right\}, \\
t_e^8 &= \max\left\{\sqrt{x_2 \bar{x}_3} M_{B_s}, \sqrt{|x_1 - x_2| \bar{x}_3} M_{B_s}, 1/b_1, 1/b_2\right\}. \quad (\text{A15})
\end{aligned}$$

They are chosen as the maximum energy scale appearing in each diagram to kill the large logarithmic radiative corrections.

- 
- [1] G. Buchalla *et al.*, Eur. Phys. J. C **57**, 309(2008) and references therein.
  - [2] A. Ali, G. Kramer and C.D. Lü, Phys. Rev. D **58**, 094009 (1998); *ibid.* **59**, 014005 (1998).
  - [3] Y.-H. Chen, H.Y. Cheng, B. Tseng, and K.C. Yang, Phys. Rev. D **60**, 094014 (1999); H.Y. Cheng and K.C. Yang, Phys. Rev. D **62**, 054029 (2000).
  - [4] M. Beneke, G. Buchalla, M. Neubert and C.T. Sachrajda, Phys. Rev. Lett. **83**, 1914 (1999); Nucl. Phys. B **591**, 313 (2000).
  - [5] Y.H. Chen, H.Y. Cheng, B. Tseng, Phys. Rev. D **59**, 074003 (1999).
  - [6] M. Beneke and M. Neubert, Nucl. Phys. B **675**, 333 (2003).
  - [7] D. Zhang, Z.J. Xiao, and C.S. Li, Phys. Rev. D **64**, 014014 (2001).
  - [8] Y. Li, C.D. Lü, Z.J. Xiao, and X.Q. Yu, Phys. Rev. D **70**, 034009 (2004); X.Q. Yu, Y. Li, and C.D. Lü, Phys. Rev. D **71**, 074026 (2005); Phys. Rev. D **73**, 017501 (2006); J. Zhu, Y.L. Shen, and C.D. Lü, J. Phys. G **32**, 101 (2006).
  - [9] Z.J. Xiao, X. Liu and H.S. Wang, Phys. Rev. D **75**, 034017 (2007).
  - [10] A. Ali, G. Kramer, Y. Li, C.D. Lü, Y.L. Shen, W. Wang and Y.M. Wang, Phys. Rev. D **76**, 074018 (2007).
  - [11] H.N. Li, S. Mishima, A.I. Sanda, Phys. Rev. D **72**, 114005 (2005).
  - [12] Z.Q. Zhang and Z.J. Xiao, arXiv: 0807.2022 [hep-ph]; arXiv: 0807.2024 [hep-ph];
  - [13] Z.J. Xiao, Z.Q. Zhang, X. Liu, and L.B. Guo, Phys. Rev. D **78**, 114001 (2008).
  - [14] H.N. Li, Prog. Part. & Nucl. Phys. **51**, 85 (2003) and references therein.
  - [15] G. Buchalla, A.J. Buras, M.E. Lautenbacher, Rev. Mod. Phys. **68**, 1125 (1996).
  - [16] C.W. Bauer, D. Pirjol, I.Z. Rothstein and I.W. Stewart, Phys. Rev. D **70**, 054015 (2004); M. Beneke and D.S. Yang, Nucl. Phys. B **736**, 34 (2006).
  - [17] T. Feldmann, P. Kroll, and B. Stech, Phys. Rev. D **58**, 114006 (1998); T. Feldmann, Int. J. Mod. Phys. A **15**, 159 (2000).
  - [18] V.M. Braun and I.E. Filyanov, Z. Phys. C **48**, 239 (1990); P. Ball, V.M. Braun, Y. Koike, and K. Tanaka, Nucl. Phys. B **529**, 323 (1998); P. Ball, J. High Energy Phys. **01**, 010 (1999).
  - [19] V.M. Braun and A. Lenz, Phys. Rev. D **70**, 074020 (2004); P. Ball and A. talbot, J. High Energy Phys. **06**, 063 (2005); P. Ball and R. Zwicky, Phys. Lett. B **633**, 289 (2006); A. Khodjamirian, Th. Mannel, and M. Melcher, Phys. Rev. D **70**, 094002 (2004).
  - [20] S. Mishima and A.I. Sanda, Prog. Theor. Phys. **110**, 549 (2003).
  - [21] E. Barberio *et al.*(Heavy Flavor Averaging Group), 0808.1297[hep-ex]; For updates see <http://www.slac.stanford.edu/xorg/hfag>.
  - [22] M. Merello (CDF Collaboration), Nucl. Phys. B (Proc.Suppl.) **170**, 39 (2007).
  - [23] Particle Data Group, C. Amsler *et al.*, Phys. Lett. B **667**, 1 (2008).
  - [24] I. Dunietz, Phys. Rev. D **52**, 3048 (1995).
  - [25] I.S. Gradshteyn and I.M. Ryzhik, Table of Integrals, Series, and Products, Academic Press, 1980.
  - [26] T. Kurimoto, H.N. Li, and A.I. Sanda, Phys. Rev. D **65**, 014007 (2001); C.D. Lu and M.Z. Yang, Eur. Phys. J. C **28**, 515 (2003).

- [27] H.N. Li and K.Ukai, *Phys. Lett. B* **555**, 197(2003).
- [28] H.N. Li and B. Melic, *Eur. Phys. J. C* **11**, 695 (1999).